THE EFFECT OF NEONATAL ADMINISTRATION OF RECOMBINANT MYOSTATIN PROPEPTIDE ON SKELETAL MUSCLE GROWTH IN MICE

A THESIS SUBMITTED TO THE GRADUATE DIVISION OF THE UNIVERSITY OF HAWAI ‘I AT MĀNOA IN PARTIAL FULFILLMENT OF THE REQUIREMENTS FOR THE DEGREE OF

MASTER OF SCIENCE

IN

ANIMAL SCIENCE

AUGUST 2018

BY

XIAOXING XU

THESIS COMMITTEE:

YONG SOO KIM, CHAIRPERSON

JINZENG YANG

BIRENDRA MISHRA

ACKNOWLEDGEMENT

This thesis would not have been possible without the guidance of several individuals who gave their assistance in the completion of this study. First, I would like to sincerely thank Dr. Yong Soo Kim for giving me the opportunity to conduct this study in his laboratory. His patience, critiques and encouragement let me know what a real researcher looks like, which will help me in the whole life of pursuing future career. I would also like to sincerely thank Dr. Jinzeng Yang who gave me support and guidance throughout my study. Furthermore, during the study, he kindly shared his laboratory experience and study methods. It really gave me a lot of inspiration and feasible solutions when I met with some unexpected difficulty. I would like to show my gratitude to Dr. Birendra Mishra who has also provided critical advice and critiques to my study. I would also like to thank my fellow colleagues in the laboratory: Arthur Wong, Hack Youn Kim and Tauyuan Soccoro. Last but not least I would like to thank my family for their unconditional love and support throughout my life.

ABSTRACT

Myostatin (MSTN) negatively regulates skeletal muscle growth by suppressing myoblast proliferation and muscle fiber hypertrophy. Effective suppression of MSTN leads to dramatic improvement of animal muscle growth. MSTN propeptide (MSTNpro) is a potent inhibitor of MSTN activity. Studies suggest that in some species like mice and rabbits, muscle fiber number is increasing during the early neonatal period. We postulated that enhancing muscle fiber hyperplasia of these animal species during early neonatal period might increase postnatal skeletal muscle growth of these animals. Therefore, the objective of this study was to examine the effect of neonatal administration of MSTNpro on skeletal muscle growth in mice. Recombinant truncated flatfish MSTNpro fused to mouse IgG Fc domain (fMSTNpro45-100mFc) was produced in *Escherichia coli (E. coli)* using pMAL-c5x expression vector and purified by the amylose and protein A affinity chromatography. About 7.52 mg of purified recombinant MBP-fMSTNpro45-100mFc was obtained from 1 L culture. The MSTN-inhibitory capacity of the purified recombinant MSTNpro was similar to that of a commercial MSTNpro produced from eukaryotic cells in a pGL3-$(CAGA)_{12}$-Luciferase repeater gene assay. In an oral administration study, eight female mice (4-month-old) were mated to two males (4-month-old), and the female mice were randomly divided into two groups: control and treatment. New-born pups in the treatment and control groups were fed with MBP-fMSTNpro45-100mFc (10 μg/g pup) and PBS, respectively, twice one day apart. The pups were weaned at 4 weeks, and their body weight were measured weekly for 7 weeks after weaning. At 11 weeks after weaning, animals were sacrificed, and gastrocnemius complex (gastrocnemius, plantaris and soleus) muscle and organ (heart, liver, spleen, kidney) samples were collected and weighed. Following the oral administration experiment, the same male and female mice were used for an intraperitoneal

administration study with the same experimental design. Newborn pups in the treatment and control groups were intraperitoneally injected MBP-fMSTNpro45-100mFc (10 μg/g pup) and PBS, respectively, on the first and second day after birth. At 10 weeks after weaning, mice were sacrificed for the muscle and organ weight. Either neonatal oral administration or intraperitoneal injection of MBP-fMSTNpro45-100mFc did not significantly affect body weight growth and gastrocnemius muscle and organ weights of mice. This result implies that the administration of MBP-fMSTNpro45-100mFc under early neonatal period did not enhance muscle hyperplasia in mice. However, this study did not examine either the transfer of recombinant MSTNpro into circulation or the muscle fiber number after the administration. Furthermore, dose-response was not examined. Further studies are needed to validate the potential of neonatal suppression of MSTN as a strategy to improve skeletal muscle growth of animals.

TABLE OF CONTENT

LIST OF TABLES

LIST OF FIGURES

LIST OF APPENDIXES

CHAPTER 1

LITERATURE REVIEW

1.1. Overview of skeletal muscle growth

1.1.1. Prenatal growth of skeletal muscle

Skeletal muscle of the vertebrate animals derives from somites, segments of paraxial mesoderm that form following an anterior–posterior progression on either side of the neural tube and notochord (Tajbakhsh and Buckingham, 1999). Specifically, the dorsal part of the somite, the dermo-myotome, gives rise to the overlying derm of the back and the skeletal muscles of the body and limbs (Buckingham et al., 2003). Myogenesis in all animals is directed, in part, by groups of transcription factors that orchestrate the processes of muscle differentiation (Baylies et al. 1998; Wigmore and Evans, 2002). In vertebrate skeletal muscles, these include myogenic regulatory factors, the basic helix-loop-helix proteins Myf5, MyoD, Myf4, and Myogenin, which play complementary roles in directing muscle development (Wigmore and Evans, 2002).

First, muscle progenitor cells delaminate from the epithelium of the hypaxial dermomyotome and migrate into the limb field, to the positions where the dorsal and ventral muscle masses will form initially (Christ and Ordahl, 1995). However, cells that migrate from the somite have not yet activated the myogenic determination genes and it is only when they reach the limb that they begin to express MyoD and Myf5 (Tajbakhsh and Buckingham, 1999). Before skeletal muscle forms, the muscle precursor cells, myoblasts, probably both before and after activation of Myf5 and MyoD, undergo extensive proliferation in the limb. Then myoblast proliferation is arrested and differentiates into myotube which depends on Myogenin and other differentiation factors like Mef2 (Buckingham et al., 2003). During this period, myotube formation occurs in two or three temporally distinct phases. The first wave of myotubes comes

from embryonic myoblasts, the second from fetal myoblasts, and they respectively give rise to the primary and secondary muscle fibers (Feldman and Stockdale, 1992). The first muscle fiber that appears is known as primary fiber, around which secondary fibers form at the time when innervation begins to be established (Ontell and Kozeka, 1984). Primary and secondary fibers can be distinguished morphologically and show some differences in muscle gene expression. It is generally believed that primary fibers mature to slow type I fibers in the adult but in entirely fast muscles, they give rise to fast type II fibers. The secondary fibers mostly mature to fast fibers in fast muscles and to either fast or slow fibers in the mixed muscles (Lefaucheur et al. 1995; Picard et al. 1995). Subsequently, the muscle masses undergo very extensive growth in the fetal period and postnatally (Buckingham et al., 2003).

1.1.2. Postnatal growth of skeletal muscle

Muscle fiber numbers are determined at around birth in most species of terrestrial vertebrates (Stickland, 1983). In bovines, the total number of muscle fibers is fixed from the end of the second trimester of gestation (180 days) (Picard et al. 1994; Gagnière et al. 1999). And the total number of fibers is considered to be established at around 95 d of gestation in pigs (Wigmore and Stickland, 1983). In birds, it is generally believed to be established before hatching (Rémignon et al., 1995). In less mature species such as the rabbit, the total number of fibers is determined during the first month after birth (Nougues, 1972). In the 1-day old rat neonate, fusing myoblasts and oriented myotubes appeared between the mononucleated cells (Oron, 1990). Fusion of myoblast to myotubes took place during the first day after birth (Oron, 1990). Therefore, although in most vertebrates, postnatal muscle growth is mostly due to hypertrophy (muscle fiber size increase), hyperplasia (muscle fiber number increase) may still occur in the early neonatal stage in some altricial species.

In birds and mammals, the large postnatal increase in muscle mass is achieved by the hypertrophy of the existing muscle fibers, and satellite cell (SC) fusion with the fibers occurs during the hypertrophy process (Grounds, 1991). SCs were first identified in 1961 (Mauro), located between the sarcolemma of the myofiber and the basal membrane (BM) (Mauro, 1961; Muir et al. 1965). They can be activated by myotrauma or excise, proliferate, self-renew, and finally differentiate into multinucleated myofibers (Hurme and Kalimo, 1992; Pavlath and Horsley, 2003; Charge´ and Rudnicki, 2004; Shi and Garry, 2006). In the neonate, SCs proliferate actively, adding nuclei to fibers (Moss and Leblond, 1971), while in the adult, they are mitotically quiescent and only become active in response to an insult or injury to the muscle (Campion, 1984).

In healthy adult animals, muscle hypertrophy is also achieved by controlling the balance of protein turnover. All muscle fibers are constantly synthesizing and degrading myofibrillar proteins, and the balance between these two processes determines whether protein content increases, decreases or remains constant. During growth, the rate of protein synthesis is greater than the rate of protein degradation, resulting in accumulation of proteins (Tipton and Wolfe, 2001). Increases in myofibril length and diameter occur as muscle fibers grow. Myofibrils grow in length by adding new sarcomeres at the ends of myofibrils and increase in diameter by adding new thick and thin filaments to the periphery of existing myofibrils. Consequently, as proteins like myosin and actin are synthesized on polyribosomes, they assemble into new filaments, and these new filaments associate with existing filaments in myofibrils. The new filaments are added to the surface of myofibrils, and they are integrated into the structure.

Degradation of muscle proteins is also a critical process in muscle growth, highly regulated and balanced with protein synthesis. It is mediated by proteolytic enzymes (Sugden

and Fuller, 1991), like calpain, caspase, lysosomal protease and the ubiquitin-dependent proteasome. Calpains are calcium-activated cysteine proteases. In vitro, calpains initiate digestion of individual myofibrillar proteins, including desmin, C-protein and tropomyosin (Huang and Forsberg, 1998). Calpains are also activated in conditions of muscle wasting, including Duchenne muscular dystrophy (Arahata and Sugita, 1989) and fasting (Arakawa et al., 1983). Calpains play a significant role in myofibrillar protein degradation, especially in the disassembly of the myofibril during early stages of turnover (Goll et al., 1989). The proteasome is also involved in myofibrillar protein degradation. The proteasome, a large, ubiquitous ATP- and ubiquitin-dependent proteolytic system, is able to degrade actin and myosin (Solomon and Goldberg, 1996). Studies also show that these two kinds of protease work synergistically in muscle protein degradation. Calpain 3, the muscle-specific calpain, contributes to protein ubiquitination (Kramerova et al., 2005), and calpain activation in myotubes increases proteasome enzyme activity (Menconi et al., 2004). The caspases, cysteine-aspartic proteases, are a family of protease enzymes playing essential roles in programmed cell death. A study indicated that the initial step in progressive loss of muscle protein in acute diabetes and renal insufficiency is activation of caspase-3, which cleaves actomyosin to its constituent proteins and fragments of these proteins, and then the resulting substrates are finally degraded in the ubiquitin-dependent proteasome system (Lee et al., 2004).

1.2. Regulators of skeletal muscle growth

1.2.1. The IGF1/PI3K/Akt and PI3K/Akt/mTOR hypertrophy signaling pathways

Muscle hypertrophy can be induced by multiple anabolic stimuli – among the most studied of which is insulin-like growth factor 1 (IGF1) (Bodine et al., 2001b; Rommel et al., 2001). Signaling via IGF1 is mediated first by IGF1 ligand binding to its receptor, the tyrosine

kinase IGF1 receptor (IGF1R). This binding induces trans-phosphorylation of the dimeric receptor, and the resultant phosphorylated tyrosines create a docking site for the recruitment of the Insulin Receptor Substrate 1 (IRS1) (Bohni et al., 1999). The IGF1 pathway can be inactivated after prolonged insulin stimulation by targeting IRS1 for ubiquitin-mediated degradation (Tzatsos and Kandror, 2006; Xu et al., 2008). Muscle-specific overexpression in transgenic mice of an IGF1 isoform locally expressed in skeletal muscle results in muscle hypertrophy (Musaro et al., 2001). Akt activation is induced by IGF1 and insulin through the generation of phosphatidylinositol-3,4,5- triphosphates produced by phosphatidylinositol 3 kinase (PI3K). The role of Akt in muscle growth was first suggested by the finding that an active Ras mutant could promote muscle growth through selective activation of the Akt pathway by PI3K (Murgia et al., 2000).

The kinase mTOR (mammalian target of rapamycin) has emerged as a key regulator of cell growth that integrates signals from growth factors, nutrients, and energy status to control protein synthesis and other cell functions (Hay and Sonenberg, 2004; Teleman et al., 2008). mTOR is part of two multiprotein complexes: mTORC1, which contains raptor and is rapamycin sensitive, is required for signaling to S6K and 4EBP1, whereas mTORC2, which contains rictor, is required for signaling to Akt-FoxO. The effect of mTOR on the translation machinery and protein synthesis is mediated by TORC1-dependent phosphorylation of the ribosomal protein S6 kinases (S6K1 and 2) and of 4E-BP1, a repressor of the cap-binding protein eIF4E (Sandri, 2008). The activation of mTOR by Akt is indirect and involves the phosphorylation and inhibition by Akt of tuberous sclerosis 2 (TSC2). The role of mTOR in muscle growth was demonstrated by in vivo studies showing that a mTOR inhibitor, rapamycin, blocked overload hypertrophy and regenerating muscle growth (Bodine et al., 2001; Pallafacchina et al., 2002).

The study found out that the activation of the Akt/mTOR pathway and its downstream targets, p70S6K and 4E-BP1, is requisitely involved in regulating skeletal muscle fiber size, and that activation of the Akt/mTOR pathway can oppose muscle atrophy induced by disuse (Bodine et al., 2001). The results suggest that activation of mTOR via PI3K/Akt serves as a crucial regulator of muscle fiber growth. A study showed the motor neuron activity on skeletal muscle growth could regenerate muscle dependent on the PI3K/Akt/mTOR pathway (Pallafacchina et al., 2002).

These studies emphasized the important role that PI3K/Akt/mTOR pathway plays in regulating skeletal muscle hypertrophy during postnatal development of animals.

1.2.2. MuRF1 and MAFbx mediated induction of muscle atrophy

In contrast to hypertrophy, skeletal muscle atrophy is characterized by a shift toward protein degradation, resulting from cachectic stimuli such as inflammatory cytokines and glucocorticoids. Proteolysis, as observed in atrophy, has been shown to occur in part due to the activation of ubiquitin-mediated proteasomal degradation (Mitch & Goldberg, 1996). Multiple models of muscle atrophy, including denervation, high-dose dexamethasone treatment, treatment with inflammatory cytokines, and simple immobilization, all induce transcriptional upregulation of MuRF1 and MAFbx (also called atrogin-1), genes that encode for E3 ubiquitin ligases (Bodine et al., 2001a; Gomes et al., 2001). A double knockout study also demonstrated that in animals there was a profound loss of type II fibers caused by MuRF1/MuRF2 interactions (Moriscot et al., 2010). MAFbx has been convincingly shown to be an E3 ligase for eIF3-f, a protein initiation factor (Li, 2007). Also, MAFbx activity results in muscle atrophy through the downregulation of protein synthesis. Activation of Akt can in turn inhibit the transcriptional upregulation of MAFbx and MuRF1 normally seen during atrophy (Ruegg and Glass, 2011). Their normal upregulation was demonstrated to require the FOXO (also known as Forkhead)

family of transcription factors (Sandri et al., 2004; Stitt et al., 2004). FOXO transcription factors are excluded from the nucleus when phosphorylated by Akt and translocate to the nucleus upon dephosphorylation (Brunet et al., 1999). The translocation and activity of FOXO transcription factors are required for upregulation of MuRF1 and MAFbx. In the case of FOXO3, the activation was demonstrated to be sufficient to induce atrophy (Mammucari et al., 2007; Zhao et al., 2007), a finding that was subsequently supported by the transgenic expression of FOXO1, which also resulted in an atrophic phenotype (McLoughlin et al., 2009; Southgate et al., 2007).

1.3. Myostatin

1.3.1. Physiology and biochemistry of myostatin

Myostatin (MSTN), also known as growth differentiation factor 8 (GDF-8), is a transforming growth factor-β (TGF-β) family member and plays an essential role in regulating skeletal muscle growth (McPherron et al., 1997). It is encoded by the *Mstn* gene. MSTN is expressed initially in the myotome compartment of developing somites and continues to be expressed in the myogenic lineage throughout development and in adult animals. Mice carrying a targeted deletion of the *Mstn* gene have a dramatic and widespread increase in skeletal muscle mass. The MSTN sequence has been highly conserved through evolution (McPherron and Lee, 1997). The human, rat, murine, porcine, turkey, and chicken MSTN sequences are similar in the biologically active C-terminal portion of the molecule (McPherron and Lee, 1997; Grobet et al., 1997; Kambadur et al., 1997; Grobet et al., 1998). MSTN is translated as a precursor protein (proMSTN) composed of a signal sequence, an N-terminal propeptide domain and a C-terminal mature (active) domain (McPherron et al., 1997; Wolfman et al., 2003). After removal of the signal peptide, the proMSTN forms a disulfide-linked homodimer and is proteolytically processed at a conserved RXRR site by the furin family of proprotein convertases to generate

propeptide and mature MSTN (Lee and McPherron, 2001; Thies et al., 2001). After cleavage, the disulfide-linked homodimer of mature MSTN is complexed with propeptide through non-covalent bond, inhibiting MSTN activity by remaining in a latent/inactive state (Hill et al., 2002; Thies et al., 2001; Zimmers et al., 2002). MSTN is activated from the latent state through cleavage of MSTNpro by members of the bone morphogenetic proteins-1/tolloid (BMP-1/TLD) of metalloproteinases (Wolfeman et al., 2003; Lee, 2008). Hence, like other TGF-β family members, MSTN is secreted and proteolytically processed as the mature form of MSTN (McPherron et al., 1997).

MSTN binds to Activin Receptor II A or B (ActRIIA or B) and Activin-Like Kinase-4 or 5 (ALK-4 or 5) (McPherron et al., 1997). The receptor binding initiates intracellular signaling via phosphorylation and activation of the transcription factors Smad2 and 3, which translocate to the nucleus and activate target genes (McCroskery et al., 2003; Rebbapragada et al., 2003). In skeletal muscle, MSTN negatively regulates Akt signaling (Sartori et al., 2009; Trendelenburg et al., 2009). Moreover, Smad2/3 inhibition promotes muscle hypertrophy partially dependent on mammalian target of rapamycin (mTOR) signaling. Thus, MSTN and Akt pathways cross-talk at different levels. These findings point to MSTN inhibitors as potential therapeutics to promote muscle growth during rehabilitation, especially when they are combined with IGF-1-Akt activators (Sartori et al., 2009). Furthermore, it has been shown that inflammatory signaling, downstream of cytokine activation, induces endogenous expression of the TGF-β family member activin, demonstrating an important interaction of cytokine and TGF-β signaling, revealing a new mechanism by which cytokines affect skeletal muscle and establishing the physiologic relevance of this pathway in the impaired regeneration seen in sarcopenia (Trendelenburg et al., 2012).

MSTN knockout mice have two- to three-fold greater muscle mass than their wild type littermates. The increased muscle mass is the result of fiber hypertrophy and hyperplasia (McPherron et al., 1997). In addition, the MSTN knockout mice accumulate less fat than their wild type littermates (McPherron and Lee, 2002; Lin et al., 2002), which may be a secondary consequence of increased muscle mass since a similar effect is seen in other genetic models of muscle hypertrophy (Musaro et al., 2001; Sutrave et al., 1990). Aside from having increased muscle and decreased fat, the MSTN knockout mice appear normal and healthy.

A similar result was also found in cattle (Grobet et al. 1997; Kambadur et al. 1997; McPherron and Lee, 1997), sheep (Clop et al., 2006), dog (Mosher et al., 2007), and human (Schuelke et al., 2004) when mutations occur in the *Mstn* gene. In 2015, researchers successfully generated MSTN-mutant Meishan pigs using Zinc Finger Nuclease technology in combination with somatic cell nucleus transfer. The MSTN-mutant pigs developed and grew normally and increased growth performance after 6 months of age with dramatic skeletal muscle mass, producing a significant amount of carcass lean tissue and less body fat (Qian et al., 2015).

1.3.2. Myostatin inhibition

Follistatin (FST) is an autocrine, secretory glycoprotein that plays a prominent role in mammalian prenatal and postnatal development. Two FST proteins with molecular weights of 32 and 35 kDa were first discovered in 1987 (Ueno et al., 1987). FST is a TGF-β binding protein, and the biological activity of FST encompasses multiple organ systems, including bone, skeletal muscle, and liver (Lin et al., 2003). MSTN can be regulated by FST, which binds the C-terminal dimer and inhibits its ability to bind to receptors. The release of the C-terminal dimer from these inhibitory proteins allows MSTN to signal through activin type II receptors (Lee and McPherron, 1997).

A gene therapy approach to MSTN inhibition represents an important consideration for patients with muscle disease. In contrast to pharmacologic administration of MSTN inhibitors such as neutralizing antibodies (Bogdanovich et al., 2002), recombinant pharmacologic agents like MSTNpro (Bogdanovich et al., 2005) or drugs such as trichostatin A (Minetti et al., 2006), gene therapy offers the convenience of a single administration of vector carrying MSTN-inhibiting gene with persistent expression for many years (Mueller and Flotte, 2008).

MSTNpro (37 kDa with glycosylation), the N-terminal part of unprocessed MSTN, has been shown to suppress MSTN bioactivity by inhibiting MSTN binding to its membrane receptor (Thies et al. 2001). Overexpression or administration of MSTNPro has been shown to enhance skeletal muscle growth in laboratory animal species (Hu et al. 2010; Lee and McPherron 1999, 2001; Li et al. 2010; Matsakas et al. 2009; Pirottin et al. 2005; Wolfman et al. 2003; Yang et al. 2001). Transgenic mice overexpressing MSTNpro showed a phenotype with enhanced muscle mass (Yang et al. 2001; Lee and McPherron, 2001; Pirottin et al., 2005). In dogs, MSTNpro overexpression via hydrodynamic limb vein injection of adeno-associated virus vector carrying the canine MSTNpro gene induced muscle hypertrophy (Qiao et al., 2009). These results showed that MSTNpro is capable of enhancing muscle growth by blockage of MSTN activity in vivo. Inhibition of MSTN function through its propeptide may also have applications to improve the growth performance of agriculturally important animals, such as pigs. The administration of mutated porcine MSTNpro to neonatal mice resulted in significant increase in growth performance (Li et al., 2010), suggesting that pharmacological inhibition of MSTN is also an effective way to improve skeletal muscle growth of animals. Moreover, transgenic mice expressing porcine MSTNpro exhibit a significant increase in body, carcass weight, and limb weight and myofiber size (Wang et al., 2013). The transgenic mice were healthy without

showing any defect. A study also showed that the administration of metalloproteinase-resistant mutant form of MSTNPro could significantly enhance skeletal muscle growth in mice (Wolfman et al. 2003). Moreover, a study has shown that both fish MSTN prodomain and FST are able to inhibit fish MSTN activity in vitro, suggesting that a similar mechanism is operating in fish as in mammals (Rebhan and Funkenstein, 2008). These results point to the potential prospects of using the two MSTN binding proteins to inhibit MSTN activity in vivo for enhancing muscle growth. A region of human MSTNpro containing residues 42–99 fully suppressed MSTN activity in co-transfection experiments. The scientists designed a series of truncation and deletion constructs of the full-length human MSTNpro including 239 amino acid residues. Each construct was co-transfected with a TGF-β-sensitive Smad-responsive luciferase reporter gene into HEK293 human embryonic kidney cells. Expression of the full-length MSTNpro-Fc fusion protein resulted in a significant reduction of MSTN-induced transcriptional activity. Then it was testified that co-transfection of each truncated MSTNpro-Fc fusion protein suppressed luciferase activity in a region-specific manner (Ohsawa et al., 2015). Compared with full-length MSTNpro, the N-terminal of the propeptide 42-99 showed almost a full capacity (98.1%) for inhibition of MSTN-induced transcriptional activity. They also identified the inhibitory core of MSTNpro consisting of 29 amino acid residues. They also demonstrated for the first time that the inhibitory core of the MSTNpro could interact with the type I and II receptors as well as the ligand by *in vitro* experiments. Similarly, a synthetic mouse MSTNpro containing residues 45–68 was effective in suppressing MSTN activity in mdx mice (Takayama et al., 2015). Also, it is shown that maltose binding protein (MBP)-fused flatfish MSTN1pro region consisting of residues 45–100 had the same MSTN inhibitory potency as the MBP-fused full sequence flatfish MSTN1pro

(Lee et al., 2016), suggesting that partial sequences of MSTNpro would be sufficient to maintain the full MSTN-inhibitory capacity.

Antibodies against MSTN has also been used to suppress MSTN activity in many studies. Blockade of endogenous MSTN by using intraperitoneal injections of blocking antibodies for three months resulted in an increase in body weight, muscle mass, muscle size and absolute muscle strength in mdx mouse muscle along with a significant decrease in muscle degeneration and concentrations of serum creatine kinase (Bogdanovich et a., 2002). The functional improvement of dystrophic muscle by MSTN blockade provides a pharmacological strategy for the treatment of diseases associated with muscle wasting such as DMD. In a study, female mice were induced to produce MSTN antibody by immunization with synthetic MSTN peptide prior to mating with male mice to examine the effect of active immunization on offspring growth and body composition (Liang et al., 2007). MSTN antibody was detected in both immunized female mice and their 8-week-old offspring. The growth performance of offspring from the MSTN antibody-induced group was higher than that from the control group at 8 weeks of age, suggesting that the induction of maternal MSTN antibody enhances the growth performance of offspring. In a 2006 study, researchers produced a monoclonal anti-MSTN antibody to examine the effects of in ovo administration of the antibody on post-hatch broiler growth and muscle mass. Eggs were injected once with monoclonal anti-MSTN antibody. Broilers from eggs that had the antibody injected into the yolk had significantly heavier body and muscle mass than the controls in both male and female birds. The results of this study indicated that immunoneutralization of MSTN during embryonic development is a potential means to improve growth potential of broilers (Kim et al., 2006). In another study, polyclonal antibodies having an affinity to chicken MSTNpro was produced , and the effect of in ovo administration of the

antibodies on post-hatch chicken growth and muscle mass was examined (Kim et al., 2007). The administration suppressed the post-hatch growth of broilers along with the decrease in muscle weight, indicating that MSTN activity was probably elevated by the binding of the antibody to the propeptide.

Treatment with an anti-MSTN antibody (ATA 842) for 4 weeks reversed age-associated sarcopenia with increased muscle strength, reduced intramuscular triglyceride content, and improved muscle insulin sensitivity in old mice (Camporez et al., 2016). A recent study demonstrated that a potent anti-MSTN antibody, mRK35 and its clinical analog, domagrozumab, were able to induce muscle anabolic activity in both rodents, including the mdx mouse model of DMD, and non-human primates (Andre et al., 2017). Specific MSTN antagonism with the human antibody REGN1033 could enhance muscle mass and function in young and aged mice, showing beneficial effects of MSTN antagonism in models of skeletal muscle atrophy (Latres et al., 2015).

Chapter 2

The effect of neonatal administration of recombinant myostatin propeptide on skeletal muscle growth in mice

2.1. Abstract

Myostatin (MSTN) negatively regulates skeletal muscle growth by suppressing myoblast proliferation and muscle fiber hypertrophy. Effective suppression of MSTN leads to dramatic improvement of animal muscle growth. MSTN propeptide (MSTNpro) is a potent inhibitor of MSTN activity. Studies suggest that in some species like mice and rabbits, muscle fiber number is increasing during the early neonatal period. We postulated that enhancing muscle fiber hyperplasia of these animal species during early neonatal period might increase postnatal skeletal muscle growth of these animals. Therefore, the objective of this study was to examine the effect of neonatal administration of MSTNpro on skeletal muscle growth in mice. Recombinant truncated flatfish MSTNpro fused to mouse IgG Fc domain (fMSTNpro45-100mFc) was produced in *Escherichia coli (E. coli)* using pMAL-c5x expression vector and purified by the amylose and protein A affinity chromatography. About 7.52 mg of purified recombinant MBP-fMSTNpro45-100mFc was obtained from 1 L culture. The MSTN-inhibitory capacity of the purified recombinant MSTNpro was similar to that of a commercial MSTNpro produced from eukaryotic cells in a pGL3-$(CAGA)_{12}$-Luciferase repeater gene assay. In an oral administration study, eight female mice (4-month-old) were mated to two males (4-month-old), and the female mice were randomly divided into two groups: control and treatment. New-born pups in the treatment and control groups were fed with MBP-fMSTNpro45-100mFc (10 µg/g pup) and PBS, respectively, twice one day apart. The pups were weaned at 4 weeks, and their body weight were measured weekly for 7 weeks after weaning. At 11 weeks after weaning, animals were

sacrificed, and gastrocnemius complex (gastrocnemius, plantaris and soleus) muscle and organ (heart, liver, spleen, kidney) samples were collected and weighed. Following the oral administration experiment, the same male and female mice were used for an intraperitoneal administration study with the same experimental design. Newborn pups in the treatment and control groups were intraperitoneally injected MBP-fMSTNpro45-100mFc (10 μg/g pup) and PBS, respectively, on the first and second day after birth. At 10 weeks after weaning, mice were sacrificed for the muscle and organ weight. Either neonatal oral administration or intraperitoneal injection of MBP-fMSTNpro45-100mFc did not significantly affect body weight growth and gastrocnemius muscle and organ weights of mice. This result implies that the administration of MBP-fMSTNpro45-100mFc under early neonatal period did not enhance muscle hyperplasia in mice. However, this study did not examine either the transfer of recombinant MSTNpro into circulation or the muscle fiber number after the administration. Furthermore, dose-response was not examined. Further studies are needed to validate the potential of neonatal suppression of MSTN as a strategy to improve skeletal muscle growth of animals.

2.2. Introduction

MSTN is a transforming growth factor-β family member and acts as a negative regulator of skeletal muscle mass. MSTN is expressed initially in the developing somites and continues to be expressed in the myogenic lineage throughout development and in adult animals. Mice carrying a targeted deletion of the MSTN gene have a dramatic and widespread increase in skeletal muscle mass (Lee and McPherron, 1997), which indicates that suppression of MSTN activity can enhance animal skeletal muscle growth. MSTNpro is an effective inhibitor of MSTN and potentially an agent for improving muscle growth of animals. Overexpression or administration of MSTNPro has been demonstrated to enhance skeletal muscle growth in some

laboratory animals (Hu et al., 2010; Lee and McPherron, 1999). Using maltose binding protein (MBP) as a fusion partner, bioactive MSTNpro was produced in soluble forms in an *E. coli* system (Lee et al., 2011; Haq et al., 2013), allowing an economic production of large quantity of an MSTN-inhibitory agent. Moreover, recent studies have shown that MBP-fused flatfish MSTN1 propeptide consisting of residues 45–100 is sufficient to maintain the full MSTN-inhibitory activity in a pGL3-$(CAGA)_{12}$-luciferase reporter assay (Lee et al., 2016), demonstrating the potential of the recombinant protein as an agent to improve skeletal muscle growth of animals via suppression of MSTN activity in vivo.

Postnatal skeletal muscle mass is determined by the embryonic muscle fiber formation and postnatal muscle hypertrophy. In most species of terrestrial vertebrates, muscle fiber number is determined at around birth (Stickland, 1983). In bovines, total muscle fiber number is fixed from the end of the second trimester of gestation (180 days) (Picard et al. 1994; Gagnière et al. 1999). The total number of fibers is considered to be established at around 95 d of gestation in pigs (Wigmore and Stickland, 1983). However, studies have indicated that muscle hyperplasia occurs during the early neonatl period in some altricial species, such as mice and rabbits (Nougues, 1972). The total fiber number in a given muscle have a permanent effect on the postnatal growth of muscles (Hegarty and Allen, 1978; Powell and Aberle, 1981; Wigmore and Stickland, 1983), suggesting that enhancing myoblast proliferation during the neonatal period of these animal species would increase the muscle mass during the postnatal growth period. Many studies have shown that MSTN suppresses myoblast proliferation (Ríos et al., 2001; Ríos et al., 2002; Seiliez et al., 2012). It is, thus, hypothesized that neonatal suppression of MSTN would increase muscle hyperplasia, leading to increased postnatal skeletal muscle growth in mice. Therefore, the objectives of the study were: (1) to express and purify a bioactive MSTNpro

protein in *E. coli*; (2) to investigate if the neonatal administration of MSTNPro affect postnatal muscle growth in mice.

2.3. Materials and Methods

2.3.1. Construction of expression vectors

An expression vector of mouse IgG Fc domain (mFc)-fused flatfish MSTN-1 propeptide containing amino acid sequences 45-100 (fMSTNpro45-100mFc) was previously constructed in Dr. Kim's laboratory. Gibson assembly cloning method was used to insert the fMSTNpro45-100 and mFc fragments into the XmnI site of pMAL-c5x expression vector (New England Biolab, MA, USA). To produce DNA fragment of fMSTNpro45-100 for Gibson assembly cloning, PCR was performed using the cDNA of full sequence flatfish MSTNpro (Lee et al., 2016) as a template. Q5 High-Fidelity DNA polymerase (New England Biolabs, MA, USA) was used with overlapping primer sets (Table 1). Mouse Fc cDNA was commercially synthesized with codon optimization and subcloned into a pUC57 cloning vector (GenScript, PA, USA). Mouse Fc fragments for Gibson cloning were produced by PCR with overlapping primer sets (Table 1) using the mouse Fc-pUC57 plasmid as a template. The overlapping primer sets were designed to contain G4S (GGTGGTGGTGGTTCT) linker between MSTNpro and Fc fragments. Each Gibson assembly reaction (New England Biolabs, MA, USA) contained approximately 100 ng of inserts and 50 ng of the XmnI-linearized *pMAL-c5x* vector, and incubated at 50°C for 30 min. After the assembly reaction, the reaction mixture was transformed into NEB 5α competent *E. coli* strain (New England Biolabs). After overnight growth at 37°C, the *pMAL-c5x-fMSTNpro45-100mFC* plasmid was extracted to confirm correct insertion by colony PCR across the assembly junctions or by DNA sequence analysis. *E. coli* strain of K12TB1 (New England Biolab, MA, USA) was transformed with the expression construct by the heat-shock method and spread on

Luria-Bertani (LB) (1.2% tryptone, 0.6% yeast extract and 0.8% NaCl, 0.2% glucose) agar plates containing 50 μg/mL ampicillin.

2.3.2. Expression of MBP-fMSTNpro45-100mFc fusion proteins in *E. coli*

The transformed *E. coli* were spread on Luria-Bertani (LB) (1.0% tryptone, 0.5% yeast extract and 0.5% NaCl) agar plates containing 100 μg/ml ampicillin. Selected colonies were used to inoculate 5 mL LB medium containing 0.2% glucose and 100 μg/ml ampicillin for overnight growth at 37°C with vigorous shaking. The 5 mL cultures were used to inoculate 25 mL LB medium containing 0.2% glucose and 100 μg/ml ampicillin, and cells were grown to an OD600 of 0.6–0.8. To induce the soluble expressions of MBP-fMSTNpro45-100mFc proteins, isopropyl-β-D-thiogalactoside (IPTG) was added to the cultures to a final concentration of 0.5 mM, and then the cultures were grown at room temperature for 4, 6, 8, 10 and 12 hrs under vigorous shaking. SDS-PAGE analysis of the cell cultures was performed to confirm the optimum expression time of the recombinant protein. The culture induced for 6 hrs expressed the highest quantity of the fusion protein sized at 75 kDa, thus 6 h induction time was selected for large-scale expressions (1 L). Finally, truncated forms of flatfish MSTN 1 prodomain (fMSTNpro45-100) fused with mouse Fc domain at C-terminal side (MBP-fMSTNpro45-100mFc) was obtained.

2.3.3. Amylose-affinity chromatography of soluble MBP-fMSTNpro45-100mFc proteins

After induction, the cell pellets were harvested by centrifugation at 4,000 g for 10 mins at 4°C. Each gram (wet weight) of cell pellets was resuspended in 5 ml of column buffer (20 mM Tris, 200 mM NaCl, 1 mM EDTA, pH 7.5). The resuspended cell solution was frozen at -20 °C overnight. After thawing in cold water, the cells were added lysozyme and DNAse and then lysed by sonication in short pulses of 15 seconds for 15 min in ice-water bath. The cell lysates

were then centrifuged at 20,000 g for 10 mins at 4°C. For each sample, the soluble fraction was collected and the same volume of column buffer was used to resuspend the insoluble fraction. SDS-PAGE analysis of the cell lysates, soluble, and insoluble fractions was performed to verify the soluble expression of the MBP-fMSTNpro45-100mFc proteins. The soluble fractions were subjected to amylose resin (New England BioLabs, MA, USA) affinity chromatography following the procedure described previously (Lee et al., 2012). Fractions were analyzed by SDS-PAGE to examine and characterize the purified proteins.

2.3.4. Protein A affinity chromatography of amylose resin affinity-purified MBP-fMSTNpro45-100mFc proteins

After amylose affinity chromatography, eluted fractions containing MBP-fMSTNpro45-100mFc proteins with high OD (OD>1.0) and eluted fractions with low OD (0.1-1.0) were pooled separately. The high OD collection and low OD collection were then subjected to protein A (Bio-Rad Laboratories, Inc., CA, USA) affinity chromatography following the procedure described previously (Hober et al., 2007). Fractions were analyzed by SDS-PAGE to examine and characterize the purified proteins.

2.3.5. Protein assay

Protein concentration was determined by the Modified Lowry Protein Assay (Thermo Scientific, CA, USA), using bovine serum albumin as a standard.

2.3.6. SDS-PAGE

SDS-PAGE was performed with 12.5% polyacrylamide gels. Samples were mixed with loading buffer containing 1.0 % β-mercaptoethanol. Protein bands were visualized by Coomassie brilliant blue staining after electrophoresis.

2.3.7. Bioactivity test for MBP-fMSTNpro45-100mFc proteins using the pGL3-$(CAGA)_{12}$-Luciferase reporter assay

As described previously (Lee et al., 2016), capacities of MBP-fMSTNpro45-100mFc proteins to inhibit MSTN activities *in vitro* were measured using the pGL3-$(CAGA)_{12}$-firefly luciferase reporter assay in HEK293 cells stably expressing $(CAGA)_{12}$-luciferase gene construct. Cells in DMEM with 10% fetal calf serum, penicillin-streptomycin plus fungizone were seeded in a 96-well culture plate (40,000 cells/well, 100 μL) and grown for 24 hrs at 37˚C with 5% CO2. One nM of MSTN (R&D Systems) plus various concentrations of commercial porcine MSTNpro (R&D Systems) or MBP-fMSTNpro45-100mFc in DMEM without serum were added to each well after removing the medium and incubated for 24 hrs. Luminescence was measured using Veritas microplate luminometer (Turner Biosystems Inc., CA, USA) after adding Bright-Glo luminescence substrate (Promega, Madison, WI, USA). The % inhibition of MSTN activity was calculated by the following formula: % inhibition = (luminescence at 1 nM MSTN— luminescence at each ligand concentration) *100/(luminescence at 1 nM MSTN– luminescence at 0 nM MSTN). The MSTN-inhibitory activities were analyzed by regression analysis using Prism 7 program (GraphPad, San Diego, CA). To examine the differences in MSTN-inhibitory capacity of the proteins, IC50 (ligand concentration inhibiting 50% of MSTN activity) values were estimated using a non-linear regression model defining dose response curve. The equation for the model was: Y = Bottom + (Top–Bottom)/ (1 + 10^(X–LogIC50)). Y is % inhibition, Bottom is the lowest value of % inhibition, Top is the highest value of % inhibition, and X is Log ligand concentration. IC50 values were analyzed by ANOVA (Analysis of Variance) using the same program.

2.3.8. Animal experiments

Oral administration of MBP-fMSTNpro45-100mFc to neonatal mice

All of the procedures of animal care and experiments were approved by IACUC , University of Hawaii at Manoa (protocol No. 16-2319-2). Eight female (4-month-old) and two male (4-month-old) B6SJLF1/J mice were housed in Small Animal Facility at 12 hr/12 hr light-dark cycles. Mice were fed with commercial rodent diet with clean water ad libitum. Four female mice were mated to each male, and the female mice were randomly divided into two groups: control and treatment. New-born pups in the treatment and control groups were fed with MBP-fMSTNpro45-100mFc (10 μg/g pup) and PBS, respectively, twice one day apart. Using a blunt pipet tip, the solution containing the recombinant proteins or PBS were delivered into the middle of the mouth for pups to swallow the solution. The pups were weaned at 4 weeks, and their body weight were measured weekly for 7 weeks after weaning. At 11 weeks after weaning, animals were sacrificed by CO_2 asphyxiation, and gastrocnemius complex (gastrocnemius, plantaris and soleus) muscle and organ (heart, liver, spleen, kidney) samples were collected and weighed.

Intraperitoneal injection of MBP-fMSTNpro45-100mFc in neonatal mice

Eight female (7-month-old) and two male (7-month-old) B6SJLF1/J mice were housed in Small Animal Facility at 12 hr/12 hr light-dark cycles. Mice were fed with commercial rodent diet with clean water ad libitum. Four female mice were mated to each male, and the female mice were randomly divided into two groups: control and treatment. Newborn pups in the treatment and control groups were intraperitoneally injected MBP-fMSTNpro45-100mFc (10 μg/g pup) and PBS, respectively, on the first and second day after birth. Mice body weight were monitored weekly for 6 weeks after weaning. At 10 weeks after weaning, mice were sacrificed by CO_2 asphyxiation and gastrocnemius complex (gastrocnemius, plantaris and soleus) muscle and organ (heart, liver, spleen, kidney) samples were collected and weighed.

2.4. Results

2.4.1. Optimization of inducible expression of MBP-fMSTNpro45-100mFc

Figure 1 shows the result of SDS-PAGE analysis of expression of MBP-fMSTNpro45-100mFc under different induction time. The construct was designed to express a 77.5 kDa protein consisting of 42.5 kDa MBP, 10 kDa fMSTNpro45-100 and 25 kDa mouse IgG Fc domain. SDS-PAGE analysis of cell lysates showed that most of the induced recombinant proteins were in the supernatant fraction, indicating that the MBP-fMSTNpro45-100mFc was mainly expressed in soluble forms. From the result, six hours of induction contained the least amount of off-target proteins compared with the other induction period, indicating that 4 h expression is the optimum induction time. The soluble fraction contained about 89 mg/L proteins with MBP-fMSTNpro45-100mFc being the highest proportion (Table 2).

2.4.2. Amylose resin affinity chromatography purification of MBP-fMSTNpro45-100mFc proteins

The soluble fraction was applied to amylose resin and eluted by the column buffer containing 10 mM maltose after washing with column buffer. When analyzed by SDS-PAGE, the elution fractions contained mostly the recombinant MBP-fMSTNpro45-100mFc proteins at 77.5 kDa with many other proteins found in the soluble fraction being removed (Fig.2). About 23.2 mg/L of MBP-fMSTNpro45-100mFc protein were purified by affinity chromatography, contributing to around 26.1% recovery from the total soluble proteins (Table 2).

2.4.3. Protein A affinity chromatography purification of MBP-fMSTNpro45-100mFc proteins

After amylose chromatography, to further purify the MBP-fMSTNpro45-100mFc proteins, eluted fractions of MBP-fMSTNpro45-100mFc with high OD (OD>1.0) and eluted

fractions with low OD (0.1-1.0) were pooled separately and subjected to Protein A column separately. As shown in Fig. 3, a majority of proteins around and below 50 kDa was removed from the affinity-purified elutions. About 7.52 mg/L of MBP-fMSTNpro45-100mFc protein (8.4% of the total proteins) was recovered by protein A affinity chromatography (Table 2).

2.4.4. Bioactivity test for the MBP-fMSTNpro45-100mFc proteins using pGL3-$(CAGA)_{12}$-Luciferase reporter assay

The purified MBP-fMSTNpro45-100mFc protein was examined for its capacity to suppress MSTN activity using the pGL3-$(CAGA)_{12}$-Luciferase reporter assay system in HEK293 cells. The commercially available MSTNpro was used as a positive control. Both commercial MSTN propeptide and MBP-fMSTNpro45-100mFc demonstrated dose-dependent inhibition of MSTN (Fig. 4). The IC_{50} value of MBP-fMSTNpro45-100mFc was not significantly different from that of commercial MSTNpro (Fig. 4), indicating that the MSTN-inhibitory potency of MBP-fMSTNpro45-100mFc is as good as the commercial MSTNpro produced in a eukaryotic expression system.

2.4.5. The effect of MBP-fMSTNpro45-100mFc protein on body weight growth of neonatal mice

Figure 5 and 6 show the body weight growth after the neonatal administration of MBP-fMSTNpro45-100mFc. The body weight growth of mice with either neonatal oral administration or intraperitoneal injection of MBP-fMSTNPro45-100mFc did not differ from that of control mice, indicating that neonatal administration of MBP-fMSTNPro45-100mFc did not influence body weight growth in mice.

2.4.6. The effect of MBP-fMSTNpro45-100mFc protein on skeletal muscle and organ weights of neonatal mice

6-7 weeks after weaning, mice were sacrificed and dissected. Gastrocnemius complex which includes gastrocnemius, soleus and plantaris muscle and organs (heart, liver, spleen, kidney and epididymal fat) were separated and weighed. Table 2 and 3 show that neither neonatal oral feeding nor neonatal intraperitoneal injection of MBP-fMSTNpro45-100mFc influenced the weights of skeletal muscle and organs.

2.5. Discussion

Expression of bioactive proteins of interest with high a quantity is very important in biological research, in which recombinant protein is designed to be used in *in vivo* animal studies. Mostly, *E. coli* is an effective host for fast cloning of target genes and expression of recombinant proteins because of its simple handling, low cost and high yields of recombinant proteins. Thus, there were some efforts to produce MSTN inhibitors, such as MSTNpro, in *E. coli*. The first trial of fish MSTNpro production in *E. coli* resulted in insoluble expression of recombinant protein (Rebhan and Funkenstein, 2008), requiring a folding process with an extremely low yield of bioactive protein. However, when MBP was used as a fusion partner, bioactive fish MSTNpro was expressed in a soluble form in *E. coli* (Lee et al., 2010). Subsequently, bioactive porcine MSTNpro was also expressed in a soluble form (Haq et al., 2013). Furthermore, various truncated forms of fish and porcine MSTNpro with comparable MSTN-inhibitory capacity were also expressed in *E. coli* (Lee et al., 2016). In this study, we used a mouse IgG Fc domain fused, truncated form of MSTNpro (MBP-fMSTNpro45-100mFc). The Fc fusion to recombinant protein is generally known to prolong the half-life of recombinant proteins. In a study, researchers constructed recombinant Factor VIII-Fc fusion protein to prolong the half-life of Factor VIII for enhanced treatment of Hemophilia A (Dumont et al., 2012). The recombinant Factor VIII-Fc fusion protein had an approximately 2-fold longer half-

life than Factor VIII without Fc in Hemophilia A mice and dogs. The extension of half-life requires the interaction of Fc with the neonatal Fc receptor (FcRn). In FcRn knockout mice, the extension of rFVIIIFc half-life is abrogated, and is restored in human FcRn transgenic mice (Dumont et al., 2012). IgG Fc domain could also facilitate purification of its fused protein by protein A column. After large amounts expression, the MBP-fMSTNpro45-100mFc proteins were purified by amylose resin and protein A column. Luciferase assay was also conducted to test the bioactivity of recombinant MSTNpro. The result showed that the biological activity of MBP-fMSTNpro45-100mFc is similar to commercial MSTNpro, efficiently suppressing MSTN activity.

After successfully expressing bioactive recombinant MSTNpro, we examined whether the administration of the recombinant MSTNpro in neonatal mice would affect their postnatal body weight and muscle growth. Previous studies indicated that muscle hyperplasia continue during the early neonatal period in some altricial species like rabbit and rat (Nougues et al., 1972; Oron, 1990), suggesting the potential of enhancing muscle hyperplasia in some species via MSTN suppression. Thus, it was postulated that the MSTNpro administration in neonatal mice would potentially increase muscle fiber number and subsequent increase in body weight and muscle growth. The newborn pups were orally fed and intraperitoneally injected with recombinant MSTNpro at the first and second day after birth. After 10 and 11 weeks, the skeletal muscle, organs and body weight data were collected. The results showed that the mass of gastrocnemius muscle and body weight were not significantly increased after the neonatal administration of recombinant MSTNpro, implying that the administration of MBP-fMSTNpro45-100mFc in the early neonatal period did not enhance muscle hyperplasia in mice. However, this study did not examine either the transfer of recombinant MSTNpro into

circulation or the muscle fiber number after the administration. Furthermore, dose-response was not examined. Further studies are needed to validate the potential of neonatal suppression of MSTN as a strategy to improve skeletal muscle growth of animals.

2.6. Conclusion

A bioactive, mouse Fc domain fused, truncated form of MSTNpro (MBP-fMSTNpro45-100mFc) was successfully produced in *E. coli* in order to examine the effect of neonatal administration of the protein on postnatal body weight and muscle growth. The neonatal administration of recombinant MSTNpro did not increase the mass of gastrocnemius muscle and body weight, implying that the administration of MBP-fMSTNpro45-100mFc in the early neonatal period did not enhance muscle hyperplasia in mice. But concluding muscle hyperplasia could not be induced by the neonatal administration of recombinant MSTNpro seems still too early. The current study did not examine if the recombinant MSTNpro is transferred into animal circulation by our administration, nor the dose-response of recombinant MSTNpro. Therefore, further studies are needed to confirm if the neonatal administration of MSTNpro can be a potential strategy to improve skeletal muscle growth of animals.

Table 1. Primer sequences used in Gibson assembly cloning

Primer	**Sequence**
Pro45-100-F	gggatcgagggaaggTGCGACTAAACGCGATCATAT
Pro45-100-R	agagccgccgccgccCAGCACGTCGTACTGGTCGAG
IgG Fc-F	gacgtgctggcggcggcggctctGGCTGTAAACCGT
IgG Fc-R	catggacatatgtgaaat**TCA**TTTGCCCGGCGAGTG

Underlined, lower case letters indicate overlapping sequences.
Red color is linker (G4S, ggcggcggcggctct).
Bold is stop codon.

	Recovery of protein per Liter *E. coli* culture (mg/L)	Yield (%)
Total soluble protein	89	100.0
Amylose affinity-purified protein	23.2	26.1
Protein A affinity-purified protein	7.52	8.4

Table 2. Yield of MBP-fMSTNpro45-100mFc recovered from each purification step

The protein concentration was measured by the Lowry protein assay using BSA as a standard.

Table 3. Muscle and organ weights in oral feeding experiments at 11 weeks

	Control		Treatment		TRT	SEX	TRT x SEX
	Female (n=17)	Male (n=12)	Female (n=12)	Male (n=9)			
Gas complex, g	0.211 (0.0049)	0.293 (0.0081)	0.221 (0.0068)	0.295 (0.0149)	NS	***	NS
Gas complex %	1.013 (0.0200)	1.142 (0.0283)	1.057 (0.0227)	1.114 (0.0656)	NS	**	NS
Liver, g	1.103 (0.0259)	1.338 (0.0503)	1.153 (0.0305)	1.194 (0.0593)	NS	**	*
Liver %	5.306 (0.0885)	5.212 (0.1407)	5.520 (0.0812)	4.840 (0.2360)	NS	**	*
Heart, g	0.110 (0.0025)	0.121 (0.0026)	0.112 (0.0016)	0.121 (0.0028)	NS	***	NS
Heart %	0.527 (0.0113)	0.474 (0.0118)	0.539 (0.0091)	0.492 (0.0164)	NS	***	NS
Kidney, g	0.331 (0.0065)	0.441 (0.0109)	0.363 (0.0088)	0.435 (0.0246)	NS	***	NS
Kidney %	1.591 (0.0246)	1.720 (0.0344)	1.737 (0.0261)	1.756 (0.0874)	*	NS	NS
Spleen, g	0.089 (0.0044)	0.090 (0.0045)	0.099 (0.0049)	0.089 (0.0047)	NS	NS	NS
Spleen %	0.421 (0.0210)	0.351 (0.0155)	0.477 (0.0261)	0.359 (0.0151)	NS	***	NS
	Male (n=12)		Male (n=9)		TRT		
Epididymal fat, g	0.305 (0.0273)		0.277 (0.0254)		NS		
Epididymal fat %	1.128 (0.1123)		1.111 (0.0880)		NS		

Data are least square means (SEM). *: P<0.05, **: P<0.01, ***: P<0.001
Gas complex, gastrocnemius complex which includes gastrocnemius, soleus and plantaris.
The muscle or organ % is relative to body weight.
Wks: Weeks

Table 4. Muscle and organ weights of mice in intraperitoneal injection experiments at 10 weeks

	Control		Treatment		TRT	SEX	TRT x SEX
	Female (n=6)	Male (n=9)	Female (n=17)	Male (n=14)			
Gas complex, g	0.221 (0.0085)	0.320 (0.0112)	0.217 (0.0053)	0.321 (0.0092)	NS	***	NS
Gas complex %	1.057 (0.0269)	1.245 (0.0219)	1.092 (0.0139)	1.281 (0.0285)	NS	***	NS
Liver, g	1.021 (0.0832)	1.285 (0.0270)	1.013 (0.0309)	1.297 (0.0415)	NS	***	NS
Liver %	4.869 (0.3488)	5.024 (0.1011)	5.116 (0.1263)	5.187 (0.1358)	NS	NS	NS
Heart, g	0.110 (0.0048)	0.118 (0.0042)	0.106 (0.0018)	0.121 (0.0027)	NS	***	NS
Heart %	0.532 (0.0289)	0.456 (0.0163)	0.535 (0.0106)	0.484 (0.0070)	NS	***	NS
Kidney, g	0.405 (0.0578)	0.424 (0.0150)	0.310 (0.0060)	0.400 (0.0164)	**	*	NS
Kidney %	1.956 (0.3227)	1.653 (0.0414)	1.570 (0.0268)	1.595 (0.0446)	*	NS	NS
Spleen, g	0.107 (0.0131)	0.086 (0.0065)	0.087 (0.0034)	0.111 (0.0149)	NS	NS	NS
Spleen %	0.519 (0.0725)	0.334 (0.0244)	0.439 (0.0184)	0.452 (0.0690)	NS	NS	NS
	Male (n=9)		Male (n=14)		TRT		
Epidydimal fat, g	0.284 (0.0432)		0.194 (0.0334)		NS		
Epidydimal fat %	1.108 (0.1724)		0.764 (0.1262)		NS		

Data are least square means (SEM). *: P<0.05, **: P<0.01, ***: P<0.001
Gas complex, gastrocnemius complex which includes gastrocnemius, soleus and plantaris.
The muscle or organ % is relative to body weight.

Wks: Weeks

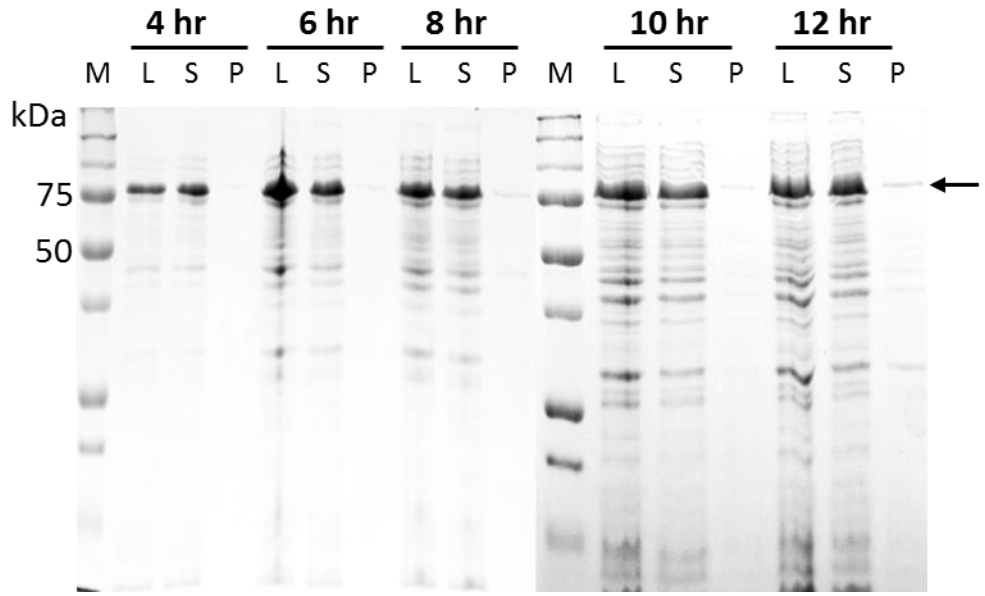

Figure 1. SDS-PAGE analysis of recombinant MBP-fMSTNpro45-100mFc expression during different induction period. To determine the optimum induction time for MBP-fMSTNpro45-100mFc expression in E. coli, culture samples were collected at 4, 6, 8, 10, and 12 hr after induction by IPTG (0.5 mM) at room temperature. Cells were collected by centrifugation, then cell pellets were lysed, followed by SDS-PAGE analysis of total lysate, soluble and insoluble fractions. Arrow indicates MBP-fMSTNpro45-100mFc. M, protein marker; L, lysate; S, supernatant; P, pellet.

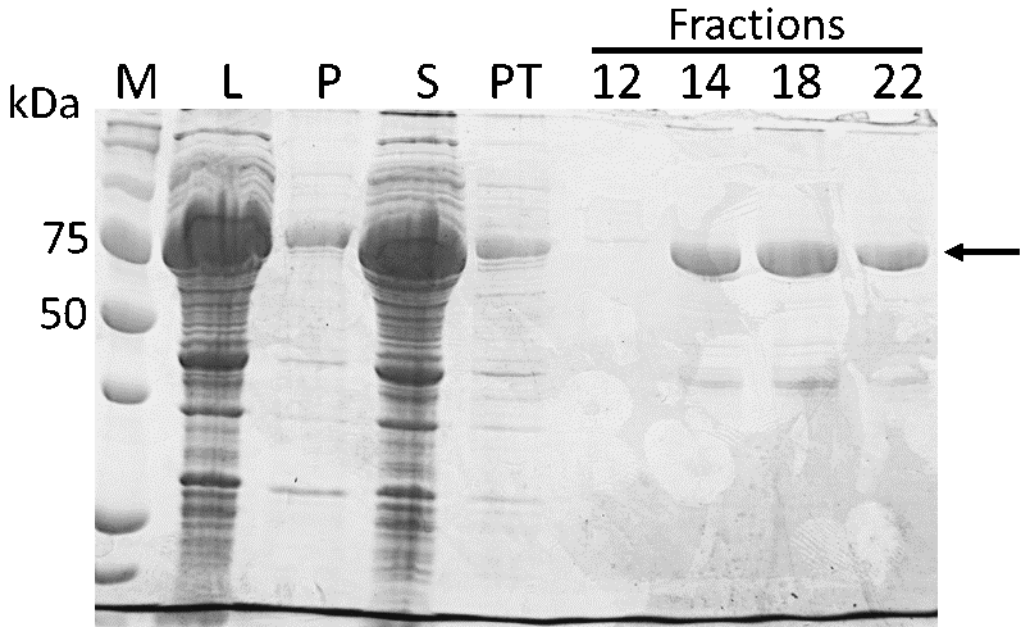

Figure 2. SDS-PAGE analysis of MBP-fMSTNpro45-100mFc purified by amylose affinity-chromatography. After 4h inducible expression at room temperature, cell pellets were collected, mixed with amylose affinity binding buffer, and lysed by sonication. The soluble fraction of lysate was collected by centrifugation and was subjected to amylose resin affinity chromatography. Elution fractions showing high OD280 were subjected to SDS-PAGE analysis. Arrow indicates amylose resin affinity-purified MBP-fMSTNpro45-100mFc. M, protein marker; L, lysate; S, supernatant; P, pellet; PT, pass-through.

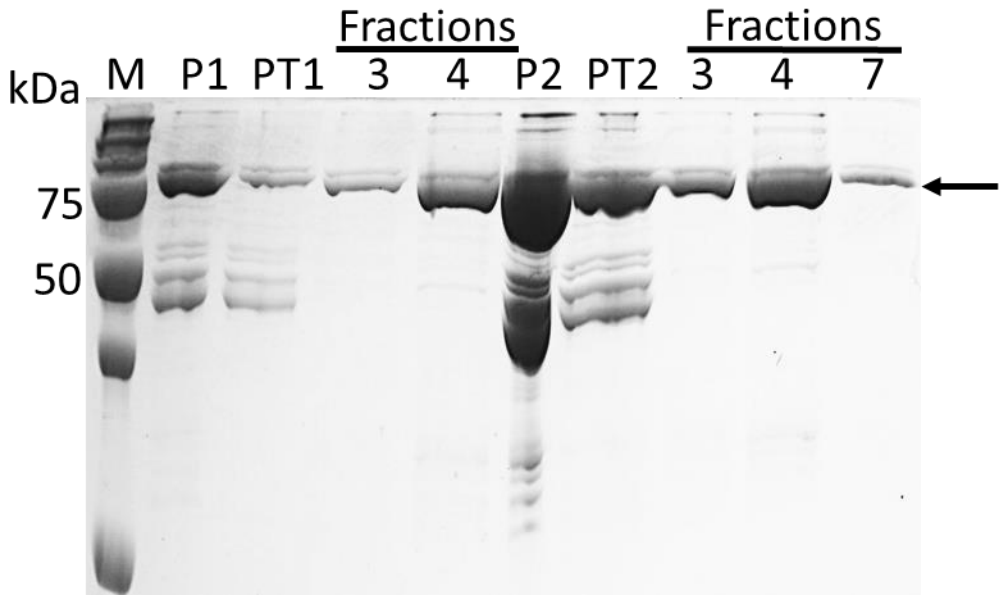

Figure 3. SDS-PAGE analysis of MBP-fMSTNpro45-100mFc purified by protein A affinity-chromatography. After amylose affinity chromatography, eluted fractions containing MBP-fMSTNpro45-100mFc with high OD (OD>1.0) and eluted fractions with low OD (0.1-1.0) were pooled separately. The high OD collection and low OD collection were then subjected to protein A affinity chromatography separately. Arrow indicates protein A affinity-purified MBP-fMSTNpro45-100mFc. M, protein marker; P1, pooled low OD (0.1-1.0) fractions of amylose-affinity purification; P2: pooled high OD (OD>1.0) fractions of amylose-affinity purification; PT, pass-through.

IC50 for 1 nM MSTN inhibition, nM

MBP-fMSTNpro45-100mFc	Commercial porcine MSTNpro
0.373^{ns}	0.449^{ns}

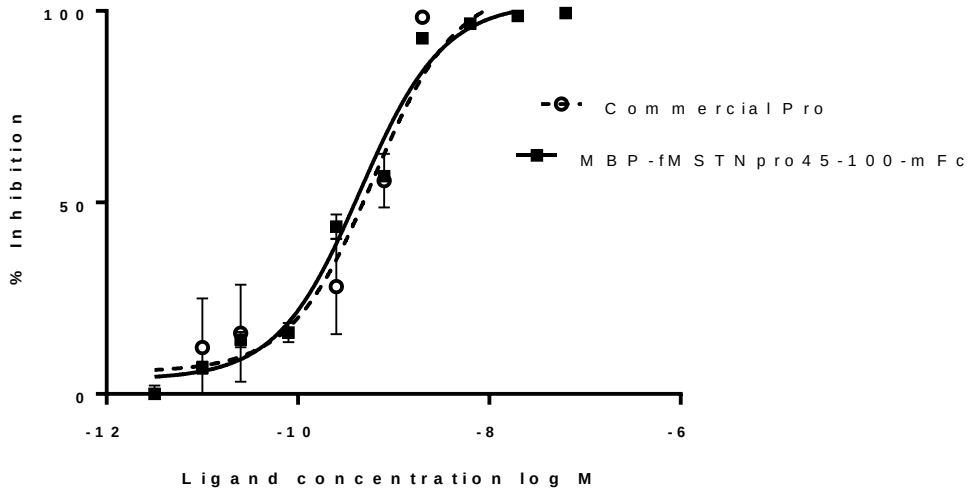

Figure 4. Inhibition of Myostatin activity by MBP-fMSTNpro45-100mFc. HEK293 cell stably expressing (CAGA)12-luciferase gene construct were used. Gradient concentrations of MBP-fMSTNpro45-100mFc in combination with 1 nM Myostatin were added to HEK293 cells, then incubated for 24 h. After that, medium was replaced by luminescence substrate and luminescence was measured. The error bars represent SEM (n = 3). NS: The means of IC50 are not significantly different.

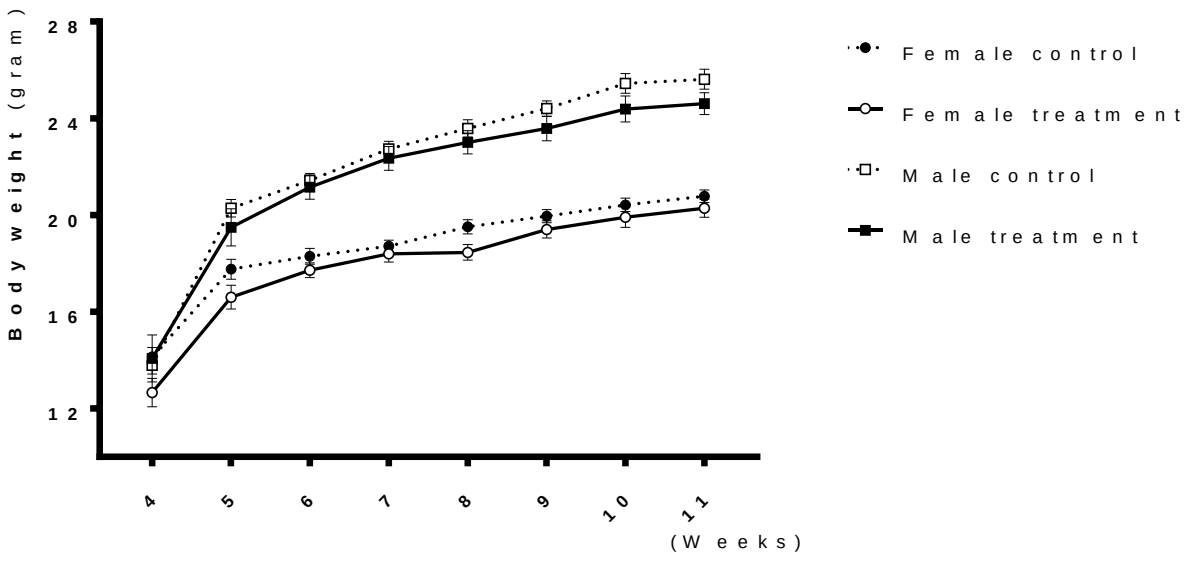

Figure 5. The effect of neonatal oral administration of MBP-fMSTNPro45-100mFc on post-weaning body weight growth. Neonatal mice in treatment groups were treated by oral feeding of 10 ug/pup MBP-fMSTNPro45-100-mFc and neonatal mice in control groups were treated by oral feeding of PBS. After 4 weeks, mice were weaned, and body weights were monitored weekly for 7 weeks.

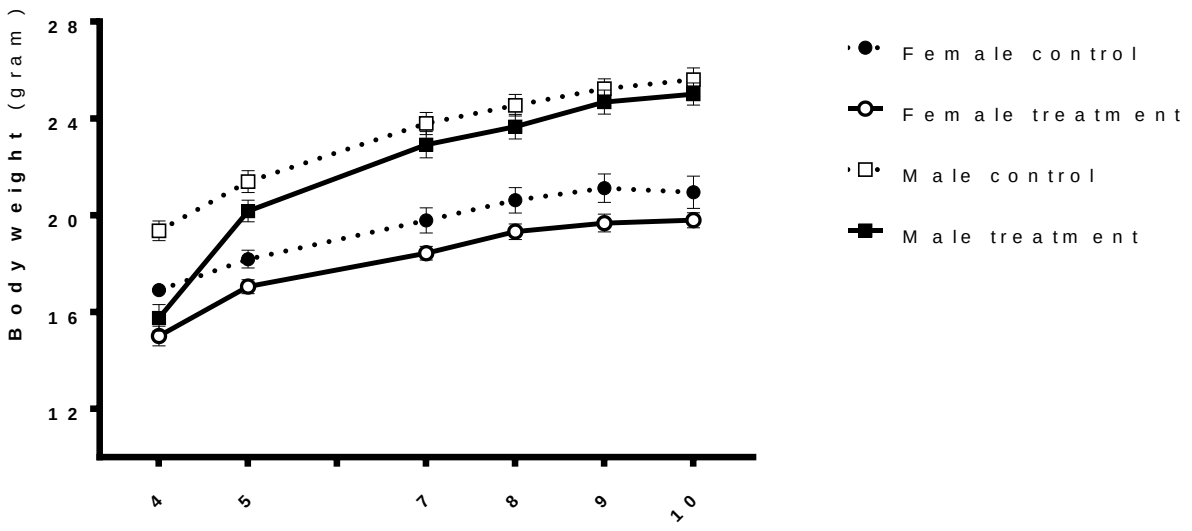

Figure 6. The effect of neonatal intraperitoneal administration of MBP-fMSTNPro45-100mFc on Post-weaning body weight growth in mice. Neonatal mice in treatment groups were treated by intraperitoneal injection of 10 ug/pup MBP-fMSTNPro45-100mFc and neonatal mice in control groups were treated by intraperitoneal injection of PBS. After 4 weeks, mice were weaned, and body weights were monitored weekly for 6 weeks.

Appendix 1. Body weight growth of mice in experiment 1 (Oral feeding)

Dam	Sire	Mouse #	Sex	Trt	4 wk	5 wk	6 wk	7 wk	8 wk	9 wk	10 wk	11 wk	Total gain
8	75	76	F	C	14.0	17.8	18.0	19.2	19.4	20.1	20.1	20.3	6.3
8	75	77	F	C	13.5	17.8	18.7	19.0	20.1	20.5	20.5	20.7	7.2
8	75	78	F	C	15.1	17.8	18.3	19.5	20.1	20.6	20.2	20.5	5.4
8	75	79	F	C	14.1	16.4	16.2	17.5	18.8	19.3	20.3	20.2	6.1
8	75	80	F	C	13.8	17.4	17.4	18.3	18.9	19.0	19.7	19.6	5.8
8	75	81	F	C	12.3	15.9	16.3	17.3	17.9	18.6	19.6	20.4	8.1
8	75	82	F	C	14.0	18.1	18.6	19.3	20.5	20.6	21.3	21.2	7.2
21	23	16	F	C	13.9	17.5	17.3	17.4	17.7	18.7	18.8	20.0	6.1
21	23	17	F	C	13.4	16.5	17.1	17.9	18.5	19.5	19.7	20.3	6.9
21	23	47	F	C	11.1	14.8	17.4	17.8	18.3	18.3	18.9	20.1	9.0
21	23	48	F	C	12.9	16.4	18.1	19.1	19.5	20.2	19.8	20.0	7.1
24	23	179	F	C	16.0	19.6	19.2	19.0	19.7	20.1	21.0	22.5	6.5
24	23	181	F	C	14.0	18.3	19.1	19.2	20.5	20.7	20.9	21.4	7.4
24	23	182	F	C	16.4	20.3	21.2	20.4	21.7	22.0	22.2	23.2	6.8
24	23	183	F	C	12.6	16.1	17.8	17.4	18.2	18.5	19.4	19.2	6.6
24	23	184	F	C	17.0	20.2	19.8	20.1	21.4	21.6	22.9	22.0	5.0
24	23	185	F	C	16.3	21.0	20.5	19.7	20.5	20.9	21.8	21.6	5.3
8	75	83	M	C	13.5	18.9	20.3	22.3	23.6	24.6	25.9	25.6	12.1
8	75	84	M	C	14.5	19.6	21.0	22.1	23.0	23.7	24.0	24.2	9.7
8	75	85	M	C	12.9	19.9	21.5	22.6	23.8	24.7	25.0	24.6	11.7
8	75	86	M	C	14.1	21.0	21.9	22.8	23.8	24.1	25.0	25.2	11.1
21	23	11	M	C	12.5	20.2	21.0	21.8	22.9	23.8	25.3	25.8	13.3
21	23	12	M	C	12.2	19.3	21.3	22.5	24.1	25.4	26.5	27.4	15.2
21	23	13	M	C	12.8	19.0	20.0	22.6	24.5	25.6	27.1	26.9	14.1
21	23	14	M	C	13.2	19.8	21.0	21.9	22.2	23.6	24.6	25.4	12.2
21	23	15	M	C	15.0	20.7	21.9	24.1	24.6	25.6	27.3	26.5	11.5
21	23	18	M	C	13.2	19.8	20.9	21.6	21.1	22.1	22.4	22.4	9.2
24	23	72	M	C	16.3	23.1	23.3	25.4	26.0	25.9	26.8	27.5	11.2
24	23	178	M	C	15.2	22.1	23.1	23.1	23.4	23.7	25.4	25.9	10.7
10	23	97	F	T	13.9	17.9	17.4	19.1	18.8	19.0	19.3	19.7	5.8
10	23	59	F	T	15.2	17.6	18.6	19.4	19.5	20.1	23.2	21.0	5.8
10	23	61	F	T	14.7	17.5	17.2	17.9	17.8	18.6	19.0	19.1	4.4
20	23	87	F	T	14.1	17.7	17.1	18.5	18.6	20.2	20.7	21.0	6.9
20	23	88	F	T	14.8	20.2	20.2	21.2	21.1	21.2	20.3	22.5	7.7
22	75	49	F	T	14.1	17.6	18.3	19.4	19.7	20.2	20.8	21.2	7.1
22	75	50	F	T	16.9	21.7	20.8	19.5	18.8	21.2	20.5	20.5	3.6
22	75	62	F	T	14.5	18.1	18.1	21.0	Sacrificed due to unexpected pregnancy				
22	75	65	F	T	13.0	16.2	16.2	17.5	18.0	21.2	20.8	21.4	8.4
22	75	66	F	T	14.2	16.7	18.4	19.8	21.3	20.2	22.1	21.4	7.2
22	75	67	F	T	13.9	17.6	17.1	17.8	18.0	20.6	20.1	20.0	6.1
22	75	68	F	T	15.1	16.9	18.3	18.4	18.0	19.6	22.0	22.5	7.4
22	75	71	F	T	12.8	16.1	16.9	17.2	18.2	20.2	19.6	20.0	7.2
9	75	152	F	T	9.4	14.5	18.6	19.3	18.9	19.6	20.1	21.5	12.1
9	75	153	F	T	9.4	15.1	17.9	17.9	18.0	18.8	20.1	20.0	10.6
9	75	155	F	T	8.8	12.9	15.2	15.1	14.9	14.6	14.5	15.3	6.5
9	75	158	F	T	9.4	14.1	17.4	17.6	17.9	18.3	18.4	18.8	9.4
9	75	159	F	T	11.4	15.8	17.6	17.6	17.6	17.8	19.5	19.6	8.2
9	75	160	F	T	8.5	13.3	15.2	15.6	17.3	18.1	18.2	18.8	10.3
9	75	162	F	T	9.1	14.6	17.8	18.2	18.3	19.2	19.1	21.1	12.0
22	75	63	M	T	14.5	18.0	18.5	21.2	21.4	21.7	22.4	23.0	8.5
10	23	89	M	T	18.2	22.9	21.8	22.6	23.6	24.1	24.4	24.7	6.5
10	23	90	M	T	18.1	22.9	23.9	24.3	24.4	25.7	26.7	27.1	9.0
10	23	91	M	T	17.2	20.5	20.5	21.0	21.8	23.0	22.6	23.6	6.4
10	23	93	M	T	17.5	22.7	23.6	25.1	25.9	26.4	Miss	26.2	8.7
10	23	96	M	T	16.9	22.7	23.5	24.2	25.1	26.5	28.3	27.3	10.4
10	23	98	M	T	17.9	22.7	23.3	24.2	25.6	25.4	27.0	25.1	7.2
20	23	92	M	T	13.9	18.1	20.4	22.9	23.5	23.7	24.9	24.6	10.7
20	23	94	M	T	13.2	18.9	18.7	18.4	19.9	19.9	21.2	21.2	8.0
9	75	151	M	T	10.7	16.8	20.6	21.0	21.6	22.4	23.3	25.4	14.7
9	75	154	M	T	10.2	16.5	20.6	22.6	22.4	22.8	23.0	23.3	13.1
9	75	156	M	T	11.1	18.5	21.9	23.1	23.3	23.2	24.2	25.0	13.9
9	75	157	M	T	8.0	14.3	19.2	20.5	21.1	22.1	23.5	24.8	16.8
9	75	161	M	T	9.6	17.4	19.6	21.7	22.5	23.2	23.7	24.8	15.2

Trt, treatment

Appendix 2. Body weight growth of mice in experiment 2 (Intraperitoneal injection)

Dam	Sire	Mouse #	Sex	Trt	4 wk	5 wk	6 wk	7 wk	8 wk	9 wk	10 wk	Total gain
22	23	116	F	C	16.7	18.8	19.4	20.5	21.4	21.6	23.5	6.8
22	23	119	F	C	17.6	18.4	19.3	19.9	20.7	22.0	21.6	4.0
22	23	121	F	C	17.4	18.1	18.6	19.3	20.5	21.3	19.8	2.4
21	75	101	F	C	16.4	17.8	18.6	19.6	21.0	22.2	19.3	2.9
198	75	488	F	C	16.3	16.7	17.2	17.8	18.2	18.3	19.7	3.4
198	75	490	F	C	17.0	19.3	19.6	21.6	21.9	21.3	21.8	4.8
22	23	117	M	C	19.0	22.1	23.8	24.3	24.9	25.3	24.6	5.6
22	23	118	M	C	16.5	19.3	20.8	21.4	22.6	23.4	23.7	7.2
22	23	120	M	C	18.9	21.0	22.7	23.7	24.5	25.3	25.0	6.1
198	75	487	M	C	20.3	21.1	21.4	23.5	24.2	24.9	25.4	5.1
198	75	489	M	C	19.2	20.2	21.1	22.9	23.7	24.5	24.5	5.3
198	75	491	M	C	20.1	22.7	24.0	25.8	26.6	26.8	27.4	7.3
198	75	492	M	C	19.5	20.2	21.4	22.6	22.9	23.7	25.0	5.5
21	75	494	M	C	20.4	22.6	23.5	25.1	25.6	26.6	27.9	7.5
21	75	493	M	C	20.3	23.3	26.4	24.8	25.9	26.5	26.9	6.6
20	75	172	F	T	14.0	16.9	18.3	20.3	21.4	20.6	21.5	7.5
20	75	169	F	T	15.7	17.9	18.1	18.7	19.6	20.0	20.7	5.0
8	23	166	F	T	15.3	16.6	16.8	18.3	19.3	19.8	19.4	4.1
8	23	165	F	T	17.4	18.9	19.0	19.8	21.5	21.6	21.3	3.9
8	23	499	F	T	16.6	18.0	18.7	18.9	20.6	21.3	21.2	4.6
8	23	483	F	T	17.2	17.8	18.0	18.7	19.5	19.7	20.7	3.5
8	23	495	F	T	17.3	18.6	18.9	19.6	20.4	20.8	20.9	3.6
8	23	486	F	T	14.8	15.8	15.0	16.8	17.6	17.8	19.0	4.2
9	23	103	F	T	12.1	15.5	21.6	18.0	18.6	18.6	18.6	6.5
9	23	104	F	T	13.9	16.8	21.6	19.0	19.5	21.3	19.3	5.4
9	23	105	F	T	15.5	16.3	21.8	17.6	18.8	19.5	19.1	3.6
9	23	107	F	T	13.3	16.0	21.8	17.6	18.9	19.2	19.1	5.8
9	23	108	F	T	16.5	18.0	23.3	19.6	20.0	20.8	20.8	4.3
9	23	110	F	T	12.6	14.9	20.3	16.0	16.8	16.7	16.7	4.1
9	23	112	F	T	15.7	18.6	23.6	19.2	19.9	20.7	20.0	4.3
9	23	113	F	T	13.2	16.8	22.1	18.4	19.0	19.3	19.8	6.6
9	23	114	F	T	14.0	16.4	22.1	16.8	17.0	16.8	18.4	4.4
20	75	174	M	T	14.0	18.7	17.7	19.8	20.7	21.1	22.3	8.3
20	75	173	M	T	15.7	19.5	21.0	22.9	23.5	24.2	24.5	8.8
20	75	164	M	T	14.7	18.1	19.6	20.8	21.6	22.7	23.0	8.3
20	75	171	M	T	16.0	20.1	21.6	22.4	22.9	24.4	25.4	9.4
20	75	170	M	T	16.3	20.4	21.7	23.7	24.2	26.9	26.4	10.1
20	75	168	M	T	16.1	21.3	22.9	24.3	25.0	26.5	26.4	10.3
20	75	167	M	T	15.4	20.9	22.2	23.9	24.5	25.1	25.2	9.8
8	23	498	M	T	18.2	20.6	21.3	23.1	23.9	25.0	25.6	7.4
8	23	497	M	T	18.8	22.8	24.2	26.6	26.6	27.1	26.8	8.0
8	23	496	M	T	18.3	22.9	24.4	25.6	26.6	26.7	27.7	9.4
8	23	484	M	T	17.0	20.0	21.5	23.0	24.2	24.7	26.2	9.2
9	23	102	M	T	12.8	17.4	22.2	19.3	20.3	22.7	22.5	9.7
9	23	106	M	T	14.5	18.8	23.0	20.3	21.2	Sacrificed due to illness		
9	23	109	M	T	15.8	21.4	26.6	23.5	24.6	25.7	25.2	9.4
9	23	111	M	T	14.9	20.4	23.0	22.3	23.9	Sacrificed due to illness		
9	23	115	M	T	11.5	18.3	24.4	21.9	22.6	22.6	22.9	11.4

Trt, treatment

Appendix 3. Muscle and organ weight of mice upon sacrifice in experiment 1

Dam	Sire	Mouse #	Sex	Trt	Gas	% Gas	Liver	% Liver	Heart	% Heart	Kidney	% Kidney	Spleen	% Spleen	Epidydimal fat	% Epidydimal fat
8	75	83	M	C	0.293	1.145	1.097	4.287	0.103	0.402	0.420	1.639	0.077	0.302	0.492	1.922
8	75	84	M	C	0.314	1.297	1.159	4.789	0.135	0.558	0.372	1.539	0.074	0.304	0.202	0.836
8	75	85	M	C	0.310	1.259	1.222	4.965	0.119	0.482	0.377	1.532	0.086	0.351	0.312	1.268
8	75	86	M	C	0.291	1.155	1.309	5.195	0.127	0.502	0.466	1.849	0.119	0.472	0.118	0.466
21	23	11	M	C	0.297	1.150	1.305	5.058	0.124	0.479	0.483	1.874	0.095	0.367	0.293	1.136
21	23	12	M	C	0.296	1.080	1.576	5.750	0.124	0.451	0.469	1.713	0.114	0.415	0.260	0.948
21	23	13	M	C	0.282	1.047	1.416	5.265	0.116	0.430	0.460	1.709	0.086	0.320	0.390	1.449
21	23	14	M	C	0.285	1.122	1.248	4.913	0.117	0.462	0.423	1.667	0.086	0.337	0.169	0.666
21	23	15	M	C	0.340	1.284	1.358	5.123	0.120	0.453	0.473	1.786	0.093	0.350	0.248	0.935
21	23	18	M	C	0.218	0.974	1.189	5.309	0.112	0.500	0.420	1.875	0.066	0.294	0.282	1.257
24	23	72	M	C	0.293	1.064	1.656	6.023	0.127	0.460	0.457	1.663	0.084	0.307	0.343	1.245
24	23	178	M	C	0.293	1.132	1.521	5.873	0.132	0.510	0.466	1.801	0.101	0.392	0.363	1.402
22	75	63	M	T	0.252	1.093	1.222	5.313	0.124	0.538	0.425	1.849	0.069	0.300	0.162	0.703
10	23	89	M	T	0.291	1.179	1.025	4.149	0.130	0.524	0.365	1.477	0.085	0.345	0.249	1.006
10	23	90	M	T	0.336	1.239	0.952	3.514	0.124	0.459	0.387	1.430	0.083	0.306	0.348	1.285
10	23	91	M	T	0.262	1.111	1.070	4.534	0.108	0.458	0.361	1.530	0.080	0.340	0.311	1.319
10	23	93	M	T	0.366	1.396	1.218	4.648	0.108	0.413	0.451	1.721	0.105	0.401	0.414	1.580
10	23	96	M	T	0.317	1.161	1.397	5.118	0.122	0.445	0.545	1.997	0.110	0.401	0.253	0.927
10	23	98	M	T	0.292	1.164	1.451	5.782	0.128	0.508	0.453	1.803	0.083	0.331	0.308	1.226
20	23	92	M	T	0.247	1.004	1.351	5.493	0.131	0.531	0.553	2.249	0.105	0.428	0.231	0.937
20	23	94	M	T	0.143	0.675	1.062	5.008	0.117	0.552	0.371	1.749	0.081	0.382	0.215	1.015
10	23	97	F	T	0.191	0.969	1.082	5.493	0.114	0.578	0.348	1.768	0.116	0.589		
10	23	59	F	T	0.232	1.104	1.249	5.949	0.113	0.537	0.374	1.781	0.102	0.486		
10	23	61	F	T	0.195	1.018	0.980	5.133	0.106	0.553	0.323	1.693	0.111	0.581		
20	23	87	F	T	0.213	1.012	1.099	5.235	0.125	0.596	0.325	1.549	0.109	0.520		
20	23	88	F	T	0.266	1.180	1.303	5.792	0.113	0.502	0.420	1.867	0.086	0.383		
22	75	49	F	T	0.210	0.989	1.110	5.237	0.109	0.514	0.357	1.682	0.108	0.510		
22	75	50	F	T	0.228	1.112	1.127	5.495	0.109	0.534	0.343	1.675	0.099	0.483		
22	75	65	F	T	0.210	0.981	1.253	5.856	0.107	0.502	0.387	1.809	0.105	0.491		
22	75	66	F	T	0.206	0.963	1.151	5.379	0.121	0.564	0.353	1.651	0.100	0.469		
22	75	67	F	T	0.211	1.055	1.082	5.408	0.108	0.538	0.363	1.814	0.052	0.259		
22	75	68	F	T	0.262	1.162	1.324	5.886	0.112	0.499	0.411	1.825	0.094	0.418		
22	75	71	F	T	0.227	1.134	1.075	5.375	0.111	0.556	0.346	1.730	0.107	0.536		
8	75	76	F	C	0.230	1.135	1.006	4.955	0.105	0.519	0.315	1.553	0.098	0.481		
8	75	77	F	C	0.215	1.037	0.972	4.693	0.112	0.543	0.333	1.607	0.093	0.449		
8	75	78	F	C	0.215	1.049	0.978	4.772	0.121	0.591	0.307	1.498	0.078	0.380		
8	75	79	F	C	0.186	0.918	1.058	5.238	0.103	0.510	0.305	1.507	0.115	0.569		
8	75	80	F	C	0.223	1.139	0.938	4.784	0.127	0.647	0.313	1.595	0.076	0.389		
8	75	81	F	C	0.172	0.841	1.059	5.190	0.095	0.466	0.292	1.432	0.098	0.479		
8	75	82	F	C	0.225	1.062	1.177	5.554	0.101	0.477	0.329	1.550	0.074	0.350		
21	23	16	F	C	0.188	0.940	1.046	5.228	0.106	0.530	0.308	1.540	0.085	0.425		
21	23	17	F	C	0.213	1.047	1.028	5.062	0.109	0.539	0.315	1.553	0.077	0.379		
21	23	47	F	C	0.183	0.912	1.094	5.444	0.103	0.514	0.328	1.630	0.058	0.289		
21	23	48	F	C	0.199	0.996	1.123	5.615	0.100	0.501	0.361	1.807	0.059	0.297		
24	23	179	F	C	0.235	1.042	1.310	5.822	0.114	0.506	0.345	1.531	0.113	0.504		
24	23	181	F	C	0.232	1.082	1.205	5.630	0.110	0.512	0.314	1.469	0.106	0.493		
24	23	182	F	C	0.214	0.924	1.259	5.428	0.131	0.563	0.391	1.685	0.105	0.451		
24	23	183	F	C	0.189	0.983	1.136	5.915	0.099	0.517	0.336	1.752	0.106	0.552		
24	23	184	F	C	0.234	1.063	1.219	5.541	0.102	0.461	0.376	1.710	0.064	0.291		
24	23	185	F	C	0.227	1.050	1.151	5.330	0.123	0.569	0.352	1.628	0.084	0.388		

Trt, treatment
Gas, gastrocnemius complex

Appendix 4. Muscle and organ weights of mice upon sacrifice in experiment 2

Dam	Sire	Mouse #	Sex	Trt	Gas	% Gas	Liver	% Liver	Heart	% Heart	Kidney	% Kidney	Spleen	% Spleen	Epidydimal fat	% Epidydimal fat
22	23	117	M	C	0.298	1.213	1.219	4.954	0.127	0.515	0.400	1.628	0.067	0.272	0.186	0.757
22	23	118	M	C	0.264	1.114	1.191	5.023	0.105	0.442	0.352	1.485	0.061	0.259	0.474	2.002
22	23	120	M	C	0.317	1.268	1.331	5.322	0.101	0.403	0.393	1.572	0.107	0.429	0.132	0.528
198	75	487	M	C	0.314	1.236	1.252	4.929	0.111	0.438	0.466	1.833	0.093	0.367	0.438	1.724
198	75	489	M	C	0.306	1.248	1.364	5.569	0.137	0.558	0.442	1.803	0.071	0.291	0.130	0.532
198	75	491	M	C	0.360	1.314	1.424	5.196	0.125	0.458	0.474	1.731	0.110	0.403	0.337	1.230
198	75	492	M	C	0.302	1.208	1.224	4.897	0.107	0.429	0.373	1.491	0.107	0.429	0.220	0.880
21	75	494	M	C	0.374	1.339	1.337	4.793	0.120	0.431	0.462	1.656	0.071	0.254	0.386	1.382
21	75	493	M	C	0.341	1.267	1.220	4.536	0.117	0.433	0.452	1.679	0.082	0.303	0.253	0.941
20	75	174	M	T	0.234	1.048	1.432	6.420	0.116	0.522	0.343	1.539	0.292	1.309	0.000	0.000
20	75	173	M	T	0.292	1.193	1.241	5.066	0.128	0.522	0.325	1.327	0.114	0.467	0.247	1.008
20	75	164	M	T	0.326	1.416	1.086	4.720	0.114	0.497	0.369	1.602	0.086	0.374	0.177	0.770
20	75	171	M	T	0.340	1.339	1.316	5.180	0.122	0.482	0.450	1.770	0.079	0.311	0.154	0.607
20	75	170	M	T	0.338	1.281	1.255	4.752	0.117	0.444	0.470	1.780	0.106	0.402	0.488	1.848
20	75	168	M	T	0.358	1.354	1.408	5.334	0.140	0.532	0.449	1.701	0.076	0.289	0.330	1.251
20	75	167	M	T	0.358	1.419	1.408	5.588	0.118	0.466	0.399	1.584	0.108	0.427	0.102	0.406
8	23	498	M	T	0.346	1.351	1.388	5.421	0.123	0.480	0.455	1.777	0.095	0.373	0.195	0.762
8	23	497	M	T	0.328	1.225	1.445	5.393	0.131	0.490	0.406	1.515	0.115	0.430	0.060	0.224
8	23	496	M	T	0.326	1.178	1.529	5.521	0.132	0.477	0.503	1.817	0.101	0.364	0.240	0.865
8	23	484	M	T	0.312	1.191	1.376	5.251	0.125	0.479	0.385	1.469	0.133	0.506	0.152	0.581
9	23	102	M	T	0.291	1.295	1.124	4.993	0.103	0.456	0.331	1.472	0.087	0.388	0.124	0.551
9	23	109	M	T	0.351	1.394	1.126	4.467	0.116	0.461	0.421	1.670	0.055	0.216	0.322	1.277
9	23	115	M	T	0.288	1.255	1.031	4.504	0.109	0.474	0.298	1.301	0.107	0.468	0.125	0.548
22	23	116	F	C	0.244	1.038	1.134	4.825	0.095	0.403	0.373	1.585	0.104	0.441		
22	23	119	F	C	0.228	1.054	0.839	3.883	0.134	0.618	0.389	1.800	0.114	0.525		
22	23	121	F	C	0.229	1.155	0.798	4.029	0.103	0.519	0.290	1.466	0.130	0.655		
21	75	101	F	C	0.206	1.065	1.017	5.267	0.106	0.548	0.685	3.551	0.153	0.793		
198	75	488	F	C	0.187	0.951	0.985	5.002	0.109	0.553	0.342	1.738	0.066	0.337		
198	75	490	F	C	0.235	1.077	1.353	6.208	0.120	0.549	0.348	1.596	0.079	0.361		
20	75	172	F	T	0.246	1.143	1.192	5.546	0.116	0.539	0.324	1.506	0.102	0.473		
20	75	169	F	T	0.224	1.080	1.177	5.686	0.115	0.556	0.326	1.572	0.087	0.419		
8	23	166	F	T	0.199	1.025	1.125	5.801	0.099	0.512	0.326	1.679	0.074	0.381		
8	23	165	F	T	0.256	1.203	1.069	5.017	0.112	0.527	0.358	1.678	0.102	0.477		
8	23	499	F	T	0.242	1.143	1.102	5.197	0.107	0.506	0.322	1.517	0.078	0.367		
8	23	483	F	T	0.216	1.044	1.156	5.583	0.107	0.516	0.341	1.645	0.093	0.448		
8	23	495	F	T	0.229	1.095	1.093	5.227	0.103	0.494	0.300	1.436	0.078	0.374		
8	23	486	F	T	0.191	1.006	1.027	5.406	0.094	0.494	0.327	1.723	0.079	0.417		
9	23	103	F	T	0.208	1.119	0.990	5.325	0.093	0.501	0.259	1.392	0.098	0.528		
9	23	104	F	T	0.205	1.062	1.029	5.331	0.094	0.489	0.291	1.508	0.092	0.476		
9	23	105	F	T	0.208	1.089	0.793	4.150	0.111	0.579	0.295	1.543	0.083	0.434		
9	23	107	F	T	0.215	1.128	0.975	5.102	0.110	0.574	0.303	1.586	0.093	0.487		
9	23	108	F	T	0.223	1.072	0.798	3.836	0.107	0.513	0.278	1.338	0.095	0.454		
9	23	110	F	T	0.168	1.007	0.866	5.184	0.105	0.628	0.279	1.671	0.071	0.423		
9	23	112	F	T	0.216	1.078	0.985	4.923	0.104	0.518	0.327	1.637	0.070	0.349		
9	23	113	F	T	0.236	1.191	1.013	5.115	0.104	0.526	0.314	1.586	0.062	0.312		
9	23	114	F	T	0.199	1.080	0.836	4.542	0.116	0.629	0.309	1.679	0.117	0.636		

Trt, treatment
Gas, gastrocnemius complex

References

Andre, M. S. et al. 2017. A mouse anti-myostatin antibody increases muscle mass and improves muscle strength and contractility in the mdx mouse model of Duchenne muscular dystrophy and its humanized equivalent, domagrozumab (PF-06252616), increases muscle volume in cynomolgus monkeys. Skeletal Muscle 7: 25.

Arahata, K., and H. Sugita. 1989. Dystrophin and the membrane hypothesis of muscular dystrophy. Trends in Pharmacological Sciences 10(11):437-439.

Arakawa, N., M. Takashima, T. Kurata, and M. Fujimaki. 1983. Effect of fasting on calcium activated protease in rat skeletal muscle. Agricultural and Biological Chemistry 47(7):1517-1522.

Baylies, M. K., M. Bate, and M. R. Gomez. 1998. Myogenesis: a view from Drosophila. Cell 93(6):921-927.

Bodine, S. C., E. Latres, S. Baumhueter, V. K.-M. Lai, L. Nunez, B. A. Clarke, W. T. Poueymirou, F. J. Panaro, E. Na, and K. Dharmarajan. 2001. Identification of ubiquitin ligases required for skeletal muscle atrophy. Science 294(5547):1704-1708.

Bodine, S. C., T. N. Stitt, M. Gonzalez, W. O. Kline, G. L. Stover, R. Bauerlein, E. Zlotchenko, A. Scrimgeour, J. C. Lawrence, and D. J. Glass. 2001. Akt/mTOR pathway is a crucial regulator of skeletal muscle hypertrophy and can prevent muscle atrophy in vivo. Nature Cell Biology 3(11):1014-1019.

Bogdanovich, S., T. O. Krag, E. R. Barton, L. D. Morris, L.-A. Whittemore, R. S. Ahima, and T. S. Khurana. 2002. Functional improvement of dystrophic muscle by myostatin blockade. Nature 420(6914):418.

Bogdanovich, S., K. J. Perkins, T. O. Krag, L.-A. Whittemore, and T. S. Khurana. 2005. Myostatin propeptide-mediated amelioration of dystrophic pathophysiology. The FASEB Journal 19(6):543-549.

Brunet, A., A. Bonni, M. J. Zigmond, M. Z. Lin, P. Juo, L. S. Hu, M. J. Anderson, K. C. Arden, J. Blenis, and M. E. Greenberg. 1999. Akt promotes cell survival by phosphorylating and inhibiting a Forkhead transcription factor. Cell 96(6):857-868.

Buckingham, M., L. Bajard, T. Chang, P. Daubas, J. Hadchouel, S. Meilhac, D. Montarras, D. Rocancourt, and F. Relaix. 2003. The formation of skeletal muscle: from somite to limb. Journal of Anatomy 202(1):59-68.

Campion, D. R. 1984. The muscle satellite cell: a review, International Review of Cytology No. 87. Elsevier. p. 225-251.

Camporez, J.-P. G., M. C. Petersen, A. Abudukadier, G. V. Moreira, M. J. Jurczak, G. Friedman, C. M. Haqq, K. F. Petersen, and G. I. Shulman. 2016. Anti-myostatin antibody increases muscle mass and strength and improves insulin sensitivity in old mice. Proceedings of the National Academy of Sciences:201525795.

Charge, S. B., and M. A. Rudnicki. 2004. Cellular and molecular regulation of muscle regeneration. Physiological Reviews 84(1):209-238.

Clop, A., F. Marcq, H. Takeda, D. Pirottin, X. Tordoir, B. Bibé, J. Bouix, F. Caiment, J.-M. Elsen, and F. Eychenne. 2006. A mutation creating a potential illegitimate microRNA target site in the myostatin gene affects muscularity in sheep. Nature Genetics 38(7):813-818.

Coleman, M. E., F. DeMayo, K. C. Yin, H. M. Lee, R. Geske, C. Montgomery, and R. J. Schwartz. 1995. Myogenic vector expression of insulin-like growth factor I stimulates muscle cell differentiation and myofiber hypertrophy in transgenic mice. Journal of Biological Chemistry 270(20):12109-12116.

Christ, B., and C. P. Ordahl. 1995. Early stages of chick somite development. Anatomy and Embryology 191(5):381-396.

Dumont, J. A., T. Liu, S. C. Low, X. Zhang, G. Kamphaus, P. Sakorafas, C. Fraley, D. Drager, T. Reidy, J. McCue, H. W. Franck, E. P. Merricks, T. C. Nichols, A. J. Bitonti, G. F. Pierce, and H. Jiang. 2012. Prolonged Activity of A Recombinant Factor VIII-Fc Fusion Protein In Hemophilia A Mice and Dogs. Blood blood-2011-08-367813.

Feldman, J. L., and F. E. Stockdale. 1992. Temporal appearance of satellite cells during myogenesis. Developmental Biology 153(2):217-226.

Goll, D. E., V. F. Thompson, R. Taylor, and J. Christiansen. 1992. Role of the calpain system in muscle growth. Biochimie 74(3):225-237.

Goll, D. E., V. F. Thompson, R. G. Taylor, and A. Ouali. 1998. The calpain system and skeletal muscle growth. Canadian Journal of Animal Science 78(4):503-512.

Gomes, M. D., S. H. Lecker, R. T. Jagoe, A. Navon, and A. L. Goldberg. 2001. Atrogin-1, a muscle-specific F-box protein highly expressed during muscle atrophy. Proceedings of the National Academy of Sciences 98(25):14440-14445.

Grobet, L., L. J. R. Martin, D. Poncelet, D. Pirottin, B. Brouwers, J. Riquet, A. Schoeberlein, S. Dunner, F. Ménissier, and J. Massabanda. 1997. A deletion in the bovine myostatin gene causes the double–muscled phenotype in cattle. Nature Genetics 17(1):71-74.

Grobet, L., D. Poncelet, L. J. Royo, B. Brouwers, D. Pirottin, C. Michaux, F. Ménissier, M. Zanotti, S. Dunner, and M. Georges. 1998. Molecular definition of an allelic series of mutations disrupting the myostatin function and causing double-muscling in cattle. Mammalian genome 9(3):210-213.

Grounds, M. 1991. Towards understanding skeletal muscle regeneration. Pathology-Research and Practice 187(1):1-22.

Haq, W. Y., S. K. Kang, S. B. Lee, H. C. Kang, Y. J. Choi, C. N. Lee, and Y. S. Kim. 2013. High-level soluble expression of bioactive porcine myostatin propeptide in E. coli. Applied Microbiology and Biotechnology 97(19):8517-8527.

Hay, N., and N. Sonenberg. 2004. Upstream and downstream of mTOR. Genes & Development 18(16):1926-1945.

Hegarty, P., and C. Allen. 1978. Effect of prenatal runting on the post-natal development of skeletal muscles in swine and rats. Journal of Animal Science 46(6):1634-1640.

Hill, J. J., M. V. Davies, A. A. Pearson, J. H. Wang, R. M. Hewick, N. M. Wolfman, and Y. Qiu. 2002. The myostatin propeptide and the follistatin-related gene are inhibitory binding proteins of myostatin in normal serum. Journal of Biological Chemistry 277(43):40735-40741.

Hu, S., C. Chen, J. Sheng, Y. Sun, X. Cao, and J. Qiao. 2010. Enhanced muscle growth by plasmid-mediated delivery of myostatin propeptide. Journal of Biomedicine and Biotechnology Volume 2010: Article ID 86259 p8.

Huang, J., and N. E. Forsberg. 1998. Role of calpain in skeletal-muscle protein degradation. Proceedings of the National Academy of Sciences 95(21):12100-12105.

Hurme, T., and H. Kalimo. 1992. Activation of myogenic precursor cells after muscle injury. Medicine and Science in Sports and Exercise 24(2):197-205.

Kambadur, R., M. Sharma, T. P. Smith, and J. J. Bass. 1997. Mutations in myostatin (GDF8) in double-muscled Belgian Blue and Piedmontese cattle. Genome Research 7(9):910-915.

Kim, Y., N. Bobbili, K. Paek, and H. Jin. 2006. Production of a monoclonal anti-myostatin antibody and the effects of in ovo administration of the antibody on posthatch broiler growth and muscle mass. Poultry Science 85(6):1062-1071.

Kim, Y., N. Bobbili, Y. Lee, H. Jin, and M. Dunn. 2007. Production of a polyclonal anti-myostatin antibody and the effects of in ovo administration of the antibody on posthatch broiler growth and muscle mass. Poultry Science 86(6):1196-1205.

Kramerova, I., E. Kudryashova, G. Venkatraman, and M. J. Spencer. 2005. Calpain 3 participates in sarcomere remodeling by acting upstream of the ubiquitin–proteasome pathway. Human Molecular Genetics 14(15):2125-2134.

Lai, K.-M. V., M. Gonzalez, W. T. Poueymirou, W. O. Kline, E. Na, E. Zlotchenko, T. N. Stitt, A. N. Economides, G. D. Yancopoulos, and D. J. Glass. 2004. Conditional activation of akt in adult skeletal muscle induces rapid hypertrophy. Molecular and Cellular Biology 24(21):9295-9304.

Latres, E., J. Pangilinan, L. Miloscio, R. Bauerlein, E. Na, T. B. Potocky, Y. Huang, M. Eckersdorff, A. Rafique, and J. Mastaitis. 2015. Myostatin blockade with a fully human monoclonal antibody induces muscle hypertrophy and reverses muscle atrophy in young and aged mice. Skeletal Muscle 5(1):34.

Lee, A. V., J. L. Gooch, S. Oesterreich, R. L. Guler, and D. Yee. 2000. Insulin-like growth factor I-induced degradation of insulin receptor substrate 1 is mediated by the 26S proteasome and blocked by phosphatidylinositol 3′-kinase inhibition. Molecular and Cellular Biology 20(5):1489-1496.

Lee, S. B., Y. S. Kim, M.-Y. Oh, I.-h. Jeong, K.-B. Seong, and H.-J. Jin. 2010. Improving rainbow trout (Oncorhynchus mykiss) growth by treatment with a fish (Paralichthys olivaceus) myostatin prodomain expressed in soluble forms in E. coli. Aquaculture 302(3-4):270-278.

Lee, S. B., M.-J. Cho, J. H. Kim, Y. S. Kim, and H.-J. Jin. 2011. Production of bioactive rockfish (Sebastes schlegeli) myostatin-1 prodomain in an Escherichia coli system. The Protein Journal 30(1):52-58.

Lee, S. B., J. H. Kim, D.-H. Jin, H.-J. Jin, and Y. S. Kim. 2016. Myostatin inhibitory region of fish (Paralichthys olivaceus) myostatin-1 propeptide. Comparative Biochemistry and Physiology Part B: Biochemistry and Molecular Biology 194:65-70.

Lee, S. B., S. K. Park, and Y. S. Kim. 2017. Maltose binding protein-fusion enhances the bioactivity of truncated forms of pig myostatin propeptide produced in E. coli. PloS One 12(4): e0174956.

Lee, S.-J., and A. C. McPherron. 2001. Regulation of myostatin activity and muscle growth. Proceedings of the National Academy of Sciences 98(16):9306-9311.

Lee, S.-J. 2008. Genetic analysis of the role of proteolysis in the activation of latent myostatin. PloS One 3(2): e1628.

Lee, S. W., G. Dai, Z. Hu, X. Wang, J. Du, and W. E. Mitch. 2004. Regulation of muscle protein degradation: coordinated control of apoptotic and ubiquitin-proteasome systems by phosphatidylinositol 3 kinase. Journal of the American Society of Nephrology 15(6):1537-1545.

Lefaucheur, L., F. Edom, P. Ecolan, and G. Butler-Browne. 1995. Pattern of muscle fiber type formation in the pig. Developmental Dynamics 203: 27-41.

Li, H.-H. et al. 2007. Atrogin-1 inhibits Akt-dependent cardiac hypertrophy in mice via ubiquitin-dependent coactivation of Forkhead proteins. The Journal of Clinical Investigation 117: 3211-3223.

Li, Z., B. Zhao, Y. S. Kim, C. Y. Hu, and J. Yang. 2010. Administration of a mutated myostatin propeptide to neonatal mice significantly enhances skeletal muscle growth. Molecular Reproduction and Development 77: 76-82.

Liang, Y.-C., J.-Y. Yeh, and B.-R. Ou. 2007. Effect of maternal myostatin antibody on offspring growth performance and body composition in mice. Journal of Experimental Biology 210(3):477-483.

Lin, J. et al. 2002. Myostatin knockout in mice increases myogenesis and decreases adipogenesis. Biochemical and Biophysical Research Communications 291: 701-706.

Lin, S.-Y., D. Phillips, and D. de Kretser. 2003. Regulation of ovarian function by the TGF-beta superfamily and follistatin. Reproduction 126: 133-148.

Lowry, O. H., N. J. Rosebrough, A. L. Farr, and R. J. Randall. 1951. Protein measurement with the Folin phenol reagent. Journal of Biological Chemistry 193: 265-275.

Mammucari, C. et al. 2007. FoxO3 controls autophagy in skeletal muscle in vivo. Cell Metabolism 6: 458-471.

Matsakas, A. et al. 2009. Molecular, cellular and physiological investigation of myostatin propeptide-mediated muscle growth in adult mice. Neuromuscular Disorders 19: 489-499.

Mauro, A. 1961. Satellite cell of skeletal muscle fibers. The Journal of Biophysical and Biochemical Cytology 9: 493-495.

McCroskery, S., M. Thomas, L. Maxwell, M. Sharma, and R. Kambadur. 2003. Myostatin negatively regulates satellite cell activation and self-renewal. The Journal of Cell Biology 162: 1135-1147.

McLoughlin, T. J. et al. 2009. FoxO1 induces apoptosis in skeletal myotubes in a DNA-binding-dependent manner. American Journal of Physiology-Cell Physiology 297: C548-C555.

McPherron, A. C., A. M. Lawler, and S.-J. Lee. 1997. Regulation of skeletal muscle mass in mice by a new TGF-β superfamily member. Nature 387: 83-90.

McPherron, A. C., and S.-J. Lee. 1997. Double muscling in cattle due to mutations in the myostatin gene. Proceedings of the National Academy of Sciences 94: 12457-12461.

McPherron, A. C., and S.-J. Lee. 2002. Suppression of body fat accumulation in myostatin-deficient mice. The Journal of Clinical Investigation 109: 595-601.

Menconi, M. J., W. Wei, H. Yang, C. J. Wray, and P.-O. Hasselgren. 2004. Treatment of cultured myotubes with the calcium ionophore A23187 increases proteasome activity via a CaMK II-caspase-calpain–dependent mechanism. Surgery 136(2):135-142.

Minetti, G., C. Colussi, R. Adami, C. Serra, C. Mozzetta, V. Parente, S. Fortuni, S. Straino, M. Sampaolesi, and M. Di Padova. 2006. Functional and morphological recovery of dystrophic muscles in mice treated with deacetylase inhibitors. Nature Medicine 12(10):1147.

Mitch, W. E., and A. L. Goldberg. 1996. Mechanisms of muscle wasting—the role of the ubiquitin–proteasome pathway. New England Journal of Medicine 335: 1897-1905.

Moriscot, A. S. et al. 2010. MuRF1 is a muscle fiber-type II associated factor and together with MuRF2 regulates type-II fiber trophicity and maintenance. Journal of Structural Biology 170: 344-353.

Mosher, D. S. et al. 2007. A mutation in the myostatin gene increases muscle mass and enhances racing performance in heterozygote dogs. PLoS Genetics 3(5): e79.

Moss, F., and C. Leblond. 1971. Satellite cells as the source of nuclei in muscles of growing rats. The Anatomical Record 170: 421-435.

Mueller, C., and T. R. Flotte. 2008. Clinical gene therapy using recombinant adeno-associated virus vectors. Gene Therapy 15(11):858.

Muir, A., A. Kanji, and D. Allbrook. 1965. The structure of the satellite cells in skeletal muscle. Journal of Anatomy 99: 435-444.

Murgia, M., A. L. Serrano, E. Calabria, G. Pallafacchina, T. Lømo, and S. Schiaffino. 2000. Ras is involved in nerve-activity-dependent regulation of muscle genes. Nature Cell Biology 2(3):142.

Musarò, A., K. McCullagh, A. Paul, L. Houghton, G. Dobrowolny, M. Molinaro, E. R. Barton, H. L. Sweeney, and N. Rosenthal. 2001. Localized Igf-1 transgene expression sustains hypertrophy and regeneration in senescent skeletal muscle. Nature genetics 27(2):195.

Nougues, J. 1972. Etude de l'évolution du nombre des fibres musculaires au cours de la croissance postnatale du muscle chez le lapin. Paris Social Biology Comptes Rendus 166(1): 165-172.

Ohsawa, Y., K. Takayama, S.-i. Nishimatsu, T. Okada, M. Fujino, Y. Fukai, T. Murakami, H. Hagiwara, F. Itoh, and K. Tsuchida. 2015. The inhibitory core of the myostatin prodomain: its interaction with both type I and ii membrane receptors, and potential to treat muscle atrophy. PloS One 10(7):e0133713.

Ontell, M., and K. Kozeka. 1984. The organogenesis of murine striated muscle: a cytoarchitectural study. American Journal of Anatomy 171(2):133-148.

Oron, U. 1990. Proteolytic enzyme activity in rat hindlimb muscles in fetus and during post-natal development. The International Journal of Developmental Biology 34(4):457-60.

Pallafacchina, G., E. Calabria, A. L. Serrano, J. M. Kalhovde, and S. Schiaffino. 2002. A protein kinase B-dependent and rapamycin-sensitive pathway controls skeletal muscle growth but not fiber type specification. Proceedings of the National Academy of Sciences 99(14):9213-9218.

Pavlath, G. K., and V. Horsley. 2003. Cell fusion in skeletal muscle: central role of NFATC2 in regulating muscle cell size. Cell Cycle 2: 419-422.

Picard, B., H. Gagnière, J. Robelin, and Y. Geay. 1995. Comparison of the foetal development of muscle in normal and double-muscled cattle. Journal of Muscle Research & Cell Motility 16: 629-639.

Picard, B., J. Robelin, F. Pons, and Y. Geay. 1994. Comparison of the foetal development of fibre types in four bovine muscles. Journal of Muscle Research & Cell Motility 15: 473-486.

Pirottin, D. et al. 2005. Transgenic engineering of male-specific muscular hypertrophy. Proceedings of the National Academy of Sciences 102: 6413-6418.

Powell, S., and E. Aberle. 1981. Skeletal Muscle and Adipose Tissue Cellularity in Runt and Normal Birth Weight Swine 1, 2. Journal of Animal Science 52(4):748-756

Qian, L. et al. 2015. Targeted mutations in myostatin by zinc-finger nucleases result in double-muscled phenotype in Meishan pigs. Scientific Reports 5: 14435-.

Qiao, C. et al. 2009. Hydrodynamic limb vein injection of adeno-associated virus serotype 8 vector carrying canine myostatin propeptide gene into normal dogs enhances muscle growth. Human Gene Therapy 20: 1-10.

Qiao, C., J. Li, J. Jiang, X. Zhu, B. Wang, J. Li, and X. Xiao. 2008. Myostatin propeptide gene delivery by adeno-associated virus serotype 8 vectors enhances muscle growth and ameliorates dystrophic phenotypes in mdx mice. Human Gene Therapy 19(3):241-254.

Rebbapragada, A., H. Benchabane, J. Wrana, A. Celeste, and L. Attisano. 2003. Myostatin signals through a transforming growth factor β-like signaling pathway to block adipogenesis. Molecular and Cellular Biology 23: 7230-7242.

Rebhan, Y., and B. Funkenstein. 2008. Inhibition of fish myostatin activity by recombinant fish follistatin and myostatin prodomain: potential implications for enhancing muscle growth in farmed fish. Aquaculture 284: 231-238.

Ríos, R., I. Carneiro, V. M. Arce, and J. Devesa. 2001. Myostatin regulates cell survival during C2C12 myogenesis. Biochemical and Biophysical Research Communications 280(2):561-566.

Ríos, R., I. Carneiro, V. M. Arce, and J. Devesa. 2002. Myostatin is an inhibitor of myogenic differentiation. American Journal of Physiology-Cell Physiology 282(5):C993-C999.

Rommel, C. et al. 2001. Mediation of IGF-1-induced skeletal myotube hypertrophy by PI (3) K/Akt/mTOR and PI (3) K/Akt/GSK3 pathways. Nature Cell Biology 3: 1009-1013.

Sandri, M. et al. 2004. Foxo transcription factors induce the atrophy-related ubiquitin ligase atrogin-1 and cause skeletal muscle atrophy. Cell 117: 399-412.

Sandri, M. 2008. Signaling in muscle atrophy and hypertrophy. Physiology 23(3):160-170.

Sartori, R. et al. 2009. Smad2 and 3 transcription factors control muscle mass in adulthood. American Journal of Physiology-Cell Physiology 296: C1248-C1257.

Schuelke, M. et al. 2004. Myostatin mutation associated with gross muscle hypertrophy in a child. New England Journal of Medicine 350: 2682-2688.

Seiliez, I., N. Sabin, and J.-C. Gabillard. 2012. Myostatin inhibits proliferation but not differentiation of trout myoblasts. Molecular and Cellular Endocrinology 351(2):220-226.

Shi, X., and D. J. Garry. 2006. Muscle stem cells in development, regeneration, and disease. Genes & Development 20: 1692-1708.

Solomon, V., and A. L. Goldberg. 1996. Importance of the ATP-ubiquitin-proteasome pathway in the degradation of soluble and myofibrillar proteins in rabbit muscle extracts. Journal of Biological Chemistry 271(43):26690-26697.

Southgate, R. J. et al. 2007. FOXO1 regulates the expression of 4E-BP1 and inhibits mTOR signaling in mammalian skeletal muscle. Journal of Biological Chemistry 282: 21176-21186.

Stickland, N. 1983. Growth and development of muscle fibres in the rainbow trout (Salmo gairdneri). Journal of Anatomy 137: 323-333.

Stitt, T. N. et al. 2004. The IGF-1/PI3K/Akt pathway prevents expression of muscle atrophy-induced ubiquitin ligases by inhibiting FOXO transcription factors. Molecular Cell 14: 395-403.

Sugden, P. H., and S. J. Fuller. 1991. Regulation of protein turnover in skeletal and cardiac muscle. Biochemical Journal 273: 21-37.

Sutrave, P., A. Kelly, and S. Hughes. 1990. ski can cause selective growth of skeletal muscle in transgenic mice. Genes & Development 4: 1462-1472.

Tajbakhsh, S., and M. Buckingham. 1999. 6 The Birth of Muscle Progenitor Cells in the Mouse: Spatiotemporal Considerations Current Topics in Developmental Biology No. 48. p 225-268. Elsevier.

Takayama, K., Y. Noguchi, S. Aoki, S. Takayama, M. Yoshida, T. Asari, F. Yakushiji, S.-i. Nishimatsu, Y. Ohsawa, and F. Itoh. 2015. Identification of the minimum peptide from mouse myostatin prodomain for human myostatin inhibition. Journal of medicinal chemistry 58(3):1544-1549.

Teleman, A. A., V. Hietakangas, A. C. Sayadian, and S. M. Cohen. 2008. Nutritional control of protein biosynthetic capacity by insulin via Myc in Drosophila. Cell metabolism 7(1):21-32.

Tipton, K. D., and R. R. Wolfe. 2001. Exercise, protein metabolism, and muscle growth. International Journal of Sport Nutrition and Exercise Metabolism 11: 109-132.

Trendelenburg, A. U., A. Meyer, C. Jacobi, J. N. Feige, and D. J. Glass. 2012. TAK-1/p38/nNFκB signaling inhibits myoblast differentiation by increasing levels of Activin A. Skeletal Muscle 2: 3.

Trendelenburg, A. U. et al. 2009. Myostatin reduces Akt/TORC1/p70S6K signaling, inhibiting myoblast differentiation and myotube size. American Journal of Physiology-Cell Physiology 296: C1258-C1270.

Tzatsos, A., and K. V. Kandror. 2006. Nutrients suppress phosphatidylinositol 3-kinase/Akt signaling via raptor-dependent mTOR-mediated insulin receptor substrate 1 phosphorylation. Molecular and Cellular Biology 26: 63-76.

Ueno, N. et al. 1987. Isolation and partial characterization of follistatin: a single-chain Mr 35,000 monomeric protein that inhibits the release of follicle-stimulating hormone. Proceedings of the National Academy of Sciences 84: 8282-8286.

Wang, K. et al. 2013. Muscle-specific transgenic expression of porcine myostatin propeptide enhances muscle growth in mice. Transgenic Research 22: 1011-1019.

Wigmore, P., and N. Stickland. 1983. Muscle development in large and small pig fetuses. Journal of Anatomy 137: 235-245.

Wigmore, P. M., and D. J. Evans. 2002. Molecular and cellular mechanisms involved in the generation of fiber diversity during myogenesis International Review of Cytology No. 216. p 175-232. Elsevier.

Wolfman, N. M. et al. 2003. Activation of latent myostatin by the BMP-1/tolloid family of metalloproteinases. Proceedings of the National Academy of Sciences 100: 15842-15846.

Xu, X. et al. 2008. The CUL7 E3 ubiquitin ligase targets insulin receptor substrate 1 for ubiquitin-dependent degradation. Molecular Cell 30: 403-414.

Yang, J. et al. 2001. Expression of myostatin pro domain results in muscular transgenic mice. Molecular Reproduction and Development: Incorporating Gamete Research 60: 351-361.

Zhao, J. et al. 2007. FoxO3 coordinately activates protein degradation by the autophagic/lysosomal and proteasomal pathways in atrophying muscle cells. Cell Metabolism 6: 472-483.

Zimmers, T. A. et al. 2002. Induction of cachexia in mice by systemically administered myostatin. Science 296: 1486-1488.